TRACK-FOLLOWING CONTROL OF HDD ACTUATOR USING H_∞ MIXED-SENSITIVITY CONTROL

TANAPOL KAEW-ARUNYIK

A THESIS SUBMITTED IN PARTIAL FULFILLMENT

OF THE REQUIREMENT FOR THE DEGREE OF

MASTER OF ENGINEERING IN DATA STORAGE TECHNOLOGY

INTERNATIONAL COLLEGE

KING MONGKUT'S INSTITUTE OF TECHNOLOGY LADKRABANG

2013

KMITL-2013-IC-M-005-017

Thesis Title	Track-Following of HDD Actuator Using H_∞ Mixed-Sensitivity Control
Student	Mr. Tanapol Kaew-Arunyik
Student ID.	52600612
Degree	Master of Engineering
Program	Data Storage Technology (International Program)
Year	2013
Thesis Advisor	Dr. Chaiwat Nuthong
Thesis Co-Advisor	Assoc. Prof. Dr. Withit Chatlatanagulchai

ABSTRACT

The prevalent trend in hard disk design tends to be smaller size hard disks with increasing larger capacities. This implies that the track width has to be smaller which leads to lower error tolerance requirement in positioning of the head. A precise control is needed for the hard disk drive (HDD) actuator; thus, controller for track-following has to achieve tighter regulation in the control of the servomechanism. In this thesis, H_∞ (H-infinity) mixed-sensitivity control method is proposed to control the track-following of the HDD actuator. It is a controller design approach that could overcome those constraints. Moreover, it is a powerful design tool for linear single-degree-of-freedom feedback systems which allows designing for performance and robustness simultaneously. This approach relies on shaping the two critical closed-loop sensitivity functions with frequency dependent weights. This thesis focuses on the controller simulation point of view and analyses the results in frequency and time domain. The problem is expressed using mathematical modeling and

simulated on MATLAB. Its performance is compared with other control methods, especially well tuned PID controller. Comparison result shows that H_∞ mixed-sensitivity method outperforms others second only CNF.

ACKNOWLEDGMENTS

I very appreciate valuable comments and advices from advisor, Dr. Chaiwat Nuthong, with kindness. I am really grateful to my work place, Seagate Technology (Thailand) for giving me the great opportunity to enhance my knowledge, experiences and also provided the scholarship.

I would especially like to thank Assoc. Prof. Dr. Withit Chatlatanagulchai for being the best co-advisor not only for instructing me in academic area but also encouraging me so that I can pass through the difficult period. This dissertation would not have been possible without him.

I would like to say many thanks to my colleges working in Asia-Engineering Drive Failure Analysis at Seagate Technology (Thailand) whose participated and shared their expertise in this thesis: Dr. Patiwat Kamonpet, Mr. Phadungsak Chusuwan for advising. I wish to convey my sincere thanks to Mr. Veerasak Phana-ngam for coordinating and cheering me up during the hard days.

Last but not least, I thank my family for their continued love and care.

Tanapol Kaew-Arunyik

TABLE OF CONTENTS

Page

TABLE OF CONTENTS (CONT.)

Page

LIST OF TABLES

Table Page

LIST OF FIGURES

LIST OF FIGURES (CONT.)

CHAPTER 1

INTRODUCTION

1.1 Background and Problem

Nowadays, the Hard Disk Drive (HDD) is the best candidate of data storage device that can support our demand with its highest capacity and reasonable price. The capacity and the size of this storage device are brought to be an important factor which affects to customer for purchasing. As the size cannot be expanded, data needs to be stored tighten and squeezed. Furthermore, Non-Repetitive Run-Out (NRRO) is the most important factor that should be considered when the mentioned constraints are done. NRRO can be defect or wear of bearing cartridge, spindle motor characteristic, external shock, or anything that does not have pattern or predictability. Thus, the hard disk drive needs a controller that can robustly compensate those unpredictable occurrences while still maintains its performance and stabilizes the system.

1.2 Literature Review

IBM has been leading the research and development of the hard disk storage technologies for a few decades. In 1973, the IBM 3340 disk storage unit, known by its internal project name "Winchester", becomes the industry standard for the next decade. The disk drive features a smaller, lighter R/W head and a ski-like design that enables the head to fly closer to the disk surface on an air of film 18 millionths of an inch thick. The areal density was about 1.7 Megabytes (MB) per square inch, compared with today's value at about tens of Gigabytes (GB) per square inch. A summary of the magnetic recording technology, including the servo technology, can be found in [1] and [2].

In [3] and [4], Tomizuka proposed an overview of the model based prediction, preview, and robust controls for motion control systems. The importance of accurate mathematical models of the controlled object and the disturbances was emphasized. He concluded that the overall performance of the actuator tracking system can be significantly improved by feedforward controls, and the model-based adaptive and/or robust controls make it be possible to realize high performance and robust of the motion control systems. [5] and [6] described design of the digital tracking controllers, and introduced the zero phase error tracking controller (ZPETC) to solve the unstable zero problems [1].

The challenges to achieve high Track-Per-Inch (TPI) were discussed in [2], [7], [8], [9], [10]. White also examined the limitation of the Track Mis-Registration (TMR) performance and the servo bandwidth due to sampling frequency and computational delays in [11].

The effects of disk modes on Position Error Signal (PES) can be found in [12] and [13]. Abramovitch Hurst and Henze published a series of paper ([14], [15], [16] and [17]) studying the TMR models. The components level breakdown methods for TMR sources were presented. In [18], Ho Hai locked the actuator to estimate sensor noise and disk modes. All these methods are based on intrusive experiments where the drive cover must be at least partially opened. Lee and Guo modeled the TMR source using only PES and inversion of the sensitivity function, and lumped all the TMR disturbances at one location [19].

The repetitive controller used to attenuating repetitive disturbances was studied in [20], [21] and [22] for the track following mode. The transient behavior of the repetitive controller was investigated in [23].

Ishikawa used an accelerometer attached to the actuator to sense the pivot friction torque to compensate for the nonlinear friction effects [24]. White and Tomizuka attached an accelerometer on the disk drive base cover and implemented an adaptive feedforward

control to reject external vibrations in [25] and [26]. In addition, several other model based adaptive friction compensation methods can be found in [27], [28], [29], and [30].

In 1995, Astrom and Wittenmark surveyed applications of adaptive control [31]. The only reference related to disk drive is [32] by Horowitz and Li. Their work on the adaptive control for disk drive track following servo are detailed in [33], [34], and [35]. Adaptive robust control (ARC) and its implementation on machine tools were presented by Yao, Al-majed, and Tomizuka in [36], [37], [38] and [39]. ARC differs from the conventional adaptive control in that it integrates the model-based robust control with the adaptation, and improves the adaptation speed.

The H_∞ Loop Shaping has been applied in [40] for track-following dual-stage actuator with 2-DOF and compared its performance to composite nonlinear feedback (CNF).

The H_∞ mixed-sensitivity control methodology was tested on a Three-Tank-System laboratory prototype [41]. The methodology is based on a stable pre-compensator and its dual post-compensator which allows solving a mixed-sensitivity problem. Frequency responses show that it is possible to shape the open loop transfer function by the control parameters. Time responses are given under flow leak, close connection valve and sensor failure.

1.3 Objectives

The H_∞ mixed-sensitivity control technique is used to carry out the design of track-following controller for an HDD with a single voice-coil motor (VCM) actuator. The model of the VCM actuator is firstly obtained then casted the overall track-following control system design into H_∞ mixed-sensitivity design framework. The simulation results of H_∞ mixed-sensitivity method is done in both time domain and frequency domain, and compared to the classical proportional-integral-derivative (PID) control technique. Furthermore, a notch filter is introduced to minimize the effect of the resonance modes with the synthesized

controller and tested for its efficacy using an illustrative simulation and the analysis on robustness. The performance of the system is done by taking the singular value responses.

1.4 Scopes

Regarding to the several constraints and requirements of the control method and performance, the scopes of this research are explained below:

1. The H_∞ mixed-sensitivity method is designed and applied base on a well-known single-stage actuator model given by Chen et al. (2006).
2. The selection of these two weight functions are normally a trial and error procedure or require detailed analysis of the system requirements.
3. The experiment will be simulated using MATLAB.
4. The experiment results yielded by H_∞ mixed-sensitivity method will be focused on performance, its robustness of track-following control and compared to other control methods.

1.5 Research Methodology

This research begins with selecting a well-known single-stage actuator model that can be used as master in which to be compared its performance when applying other control methods. Several constraints and requirements of the control design will then be defined. After getting the final requirements of the design, the plant will be formulated as an H_∞ optimization problem which can be posed under a general configuration for building up the generalized plant. As the name of the control method implied, mixed-sensitivity, the sensitivity and its complementary function are added as weight functions in the configuration in order to shape the signal under their boundary until it meets the requirements as the following steps are summarized.

1. Choose a nominal model with low order G(s).

2. Estimate the multiplicative output uncertainty of the system with respect to the chosen nominal model.

3. Define requirement of the controller design.

4. Using an empirical formula to initiate the weight functions.

5. Build up the augmented plant and synthesize the controller

6. Try to adjust parameters in the empirical formula until obtaining the desired behavior of the temporal response.

1.6 Research Overview

This research is divided into five chapters. Chapter 1 is the current chapter which introduces the research topic and summarizes the details on the literature reviewed earlier before commencing on the adaptation stage. In the last of this chapter explains on the objectives, scopes and methodology of the research.

The following Chapter 2 will focus on the theoretical explanation of a well-known single-stage actuator and its transfer function including diagram of overall control system.

Next, in Chapter 3 will explain about principle of H_∞ mixed-sensitivity control method which will be applied to the mentioned actuator model in Chapter 2.

After the proposed control method is explained in Chapter 3, a simplified design methodology of the weighting functions is proposed and initiated for simulation in Chapter 4.

Finally, the conclusion will be made in Chapter 5 by concluding the overall results obtained as well as the knowledge learned from this research.

CHAPTER 2

BACKGROUND THEORY

2.1 HDD Mechanical Structure and Its Components

The mechanical structure and its components are shown in Figure 2.1. A brief description is given below:

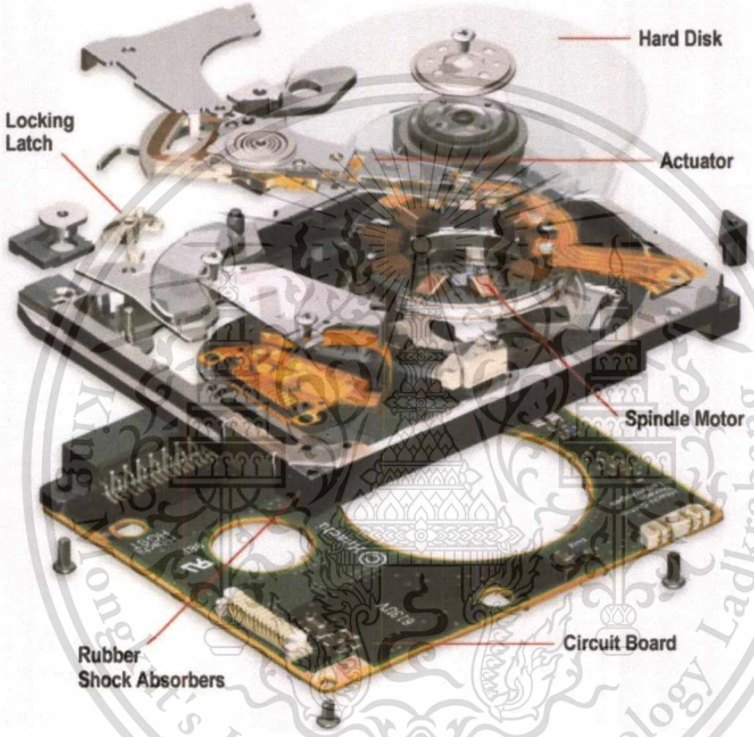

Figure 2.1 Mechanical structure of a typical HDD [42]

The most important component is Device Enclosure as it is used to determine the HDD reliability and helps to keep the contamination low. The remaining dust or particle blows inside the enclosure with the designed air turbulence, with the aid of recirculation and a breather filter, they keep out dust and other contamination that could enter between the R/W heads and platters or media over which they float and reduces the possibility of head crashes. The two major parts, the motor base assembly and top cover, are sealed with

a gasket. The motor base assembly provides supports for the spindle, actuator, VCM yoke and electronics card.

Typical hard disk has one or more disks, each with two magnetic surfaces, called platters or media. These are made of either an Al-Mg alloy substrate material electrolyses plated with Ni-P, or a mixture of glass and ceramic. The magnetic material, to allow data storage, is applied as a thin coating on both sides of each platter together with a carbon overcoat. The surfaces of each platter are precision machined and treated to remove any imperfections, and attention is paid during the manufacturing process to ensure a very smooth surface.

Actuator Assembly consists of a VCM, printed circuit cable data flex cable, actuator arms and crash-stops at both ends of travel. The data are read/written from/to the platters using the read/write (R/W) heads mounted on the top and bottom surfaces of each platter. The heads are supported by the actuator arm. The actuator in HDDs, i.e. the VCM actuator, the name implies that it works like a loud speaker. The electrical input to the VCM is energized through a flex cable. The coil of the VCM actuator extends between magnets. The write-driver/preamplifier is often part of the actuator assembly, which is mounted on the printed circuit cable.

The R/W heads are made of ferrite, metal-in-gap, thin-film or magnetoresistive (MR) types. Older types, i.e. ferrite, metal-in-gap, and thin film, used the principle of electromagnetic induction, whereas the modern disk drive heads use MR heads, which use the principle of change of magnetoresistance. Both read and write operations in older disk drives were performed by a single head, but the modern HDDs use separate heads for read and write operations. These heads are positioned only microinches above the recording medium on an air-bearing surface, which is often referred to as a slider. A gimbal attaches the slider to a stainless steel suspension to allow for pitch and roll, and the suspension is attached to the arm of the actuator by a ball swaging as shown in Figure 2.2.

All hard disks use servo-controlled direct-current (DC) spindle motors and are configured for direct connection. There are no belts or gears used to connect them to the hard disk platter spindle. The critical component of the hard disk's spindle motor is the set of spindle motor bearings at each end of the spindle shaft. These bearings are used to turn the platters smoothly. All of modern hard disk drive models usually use fluid dynamic bearing (FDB) rather than the old style metal ball bearing. The disk clamper and spacers are other important parts of this assembly.

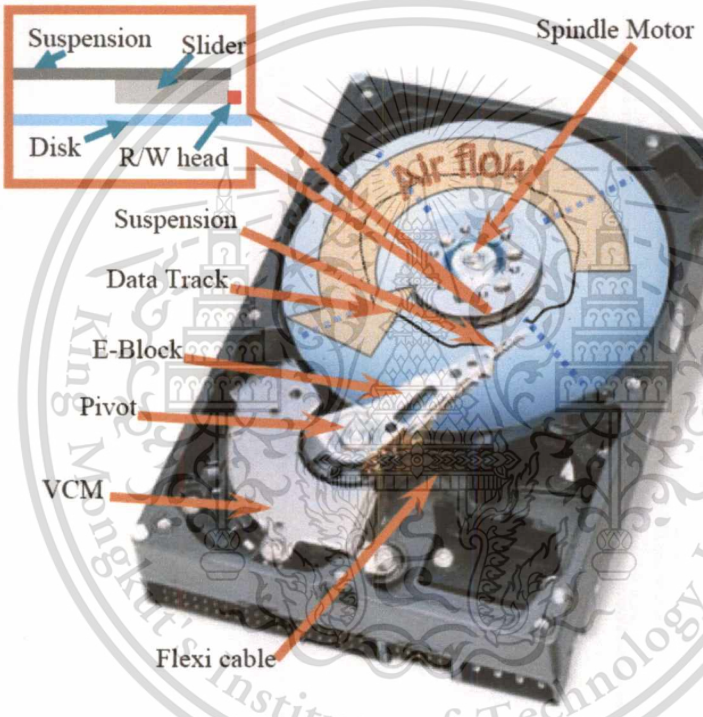

Figure 2.2 Schematic of a typical modern hard disk drive [43]

The printed circuit board provides an interface to the host personal computer (PC). The most common interfaces used are the integrated drive electronics (IDE), the advanced technology attachment (ATA), and the small computer systems interface (SCSI), which all use integrated electronic circuits. These integrated circuits have a power driver for the spindle motor, VCM, R/W electronics, servo demodulator, controller chip for timing control and control of interface, microcontroller/digital signal processor (DSP) for servo control and control interface, ROM and RAM for firmware and data transfer.

2.2 HDD Servo Systems

The HDD servo system consists of two parts: the spindle motor servo system, and the actuator servo system. Both are real-time embedded systems. The disks rotate at a constant speed and the actuator moves over the disk surface. The task of the spindle servo is to keep the constant rotation speed. Historically, the spindle servo system has been well designed. This thesis is mainly concerned with the actuator servo system

The servo system calculates voltage command based on position error signals (PES) demodulated from servo sectors. The voltage command is then fed through an analog power amplifier (PA) via a digital to analog converter (DAC). The DAC acts as a zero-order hold (ZOH). The output current of PA passes the coils of the VCM, and the resulted torque drives the actuator for track following and seeking.

Figure 2.3 illustrates the widely used embedded servo scheme for HDDs. In the scheme, position signals are embedded in the servo sectors along the data tracks at equally spaced angles, with data sectors in between. R/W head reads sector number, track ID, and PES from the servo sectors. The number and the width of the servo sectors should be minimized for data format efficiency of HDDs. Servo sectors are pre-written on the disk before the disk can be used. Servo writing is performed by precision servo writers. Because the servo system uses the heads and servo sectors as the position sensor, the servo writers must achieve much higher positioning accuracy than the HDD servo system can do.

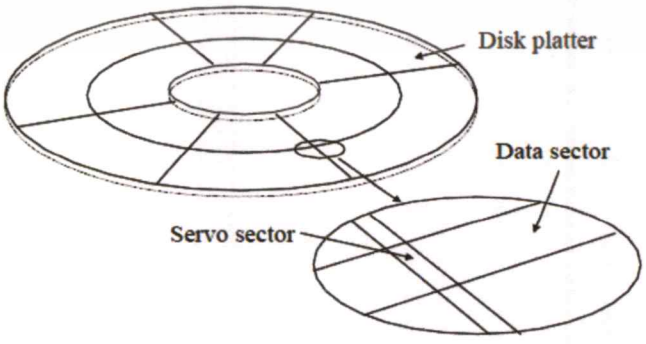

Figure 2.3 Servo sector and data sector in embedded servo system [44]

Servo sectors provide R/W heads position information; data sectors store user data. The number of servo sectors per revolution and spindle speed determines the sampling rate. Referred to Figure 2.3, only 6 servo and data sectors are shown for illustration purpose. Commercial HDDs normally have more than a hundred sectors.

Figure 2.4 shows a simplified scheme of a servo sector. Assuming the head is moving from the left to the right, written in the servo sector are the sector address mark (SAM), gray code, ABCD bursts and optional repeatable runout (RRO) fields. SAM signals a coming servo sector and also indicates the sector number. The gray code provides the track number. Group of magnetic written-in patterns with certain radial offsets are called "Bursts". Each burst group has the width of a track. The position of the R/W head can be determined by the difference of the signal strength read back from these burst groups (A and B bursts shown). The relationship between the burst amplitude read back by the head and position of the head from the track center is given as where W_r is the width of the read head; V_a and V_b are the amplitude of the A and B bursts read back by the head; V_m is the maximum amplitude for the bursts. Ideally, V_a and V_b should be a constant.

$$\Delta y_{pes} = W_r \frac{v_a - v_b}{2v_m} \tag{2.1}$$

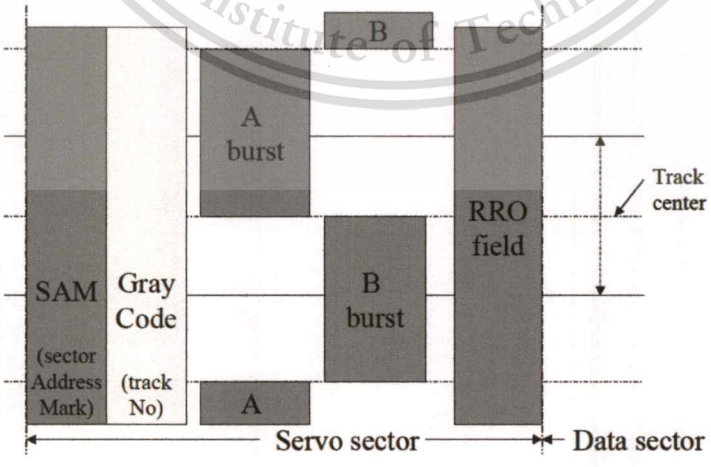

Figure 2.4 Schematic of a servo sector [44]

Note that in this two-burst scheme, the maximum detectable position error is 25% of the track width. Usually, two or more bursts are used to increase the dynamic range and linearity of the PES. Optional RRO fields at the end of the servo sector can be used to store relevant information to correct the eccentricity of the servo sector center. Because the bursts are written by the servo writer, their radial positions also reflect the tracking errors. Normally, the center of the bursts will not form as a perfect circle. However, being the only position information sources in HDD, they are the reference trajectory for the R/W head to follow. The offsets of the bursts from a perfect circle are called servo written-in errors, which are deterministic and different for each track. Figure 2.5 shows a typical scheme to convert the analog signals read from the bursts to PES. The analog signals are conditioned by an adaptive filter then sent to an analog-to-digital converter (ADC). The adaptive filter is not only be used to attenuate the undesired media and electronic noises, but also anti-alias high-frequency noise. The servo digital signal processor (DSP) processes the results in digital format, and computes PES.

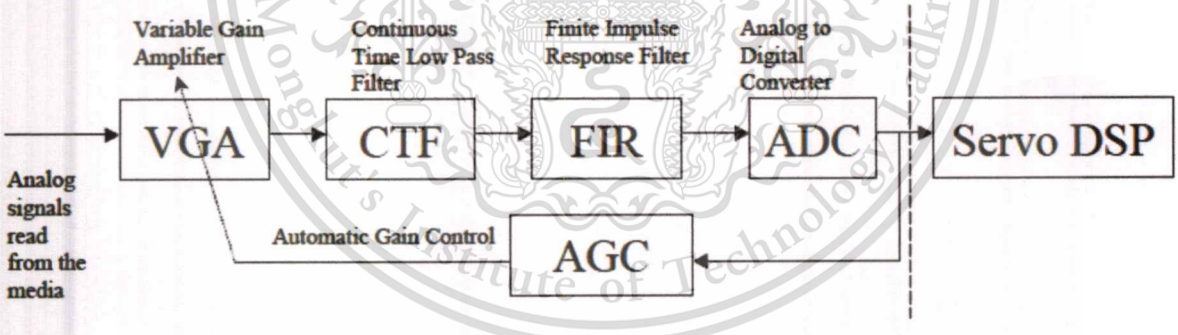

Figure 2.5 A typical hard disk drive read channel scheme [44]

In HDD, data are stored in tightly-packed concentric rings called tracks, and organized for fast access. Each track is further divided into smaller sectors. The stored data are located by the cylinder, head, and sector numbers, which are provided to the servo subsystem by the controller interface when the data are acquired by a host computer.

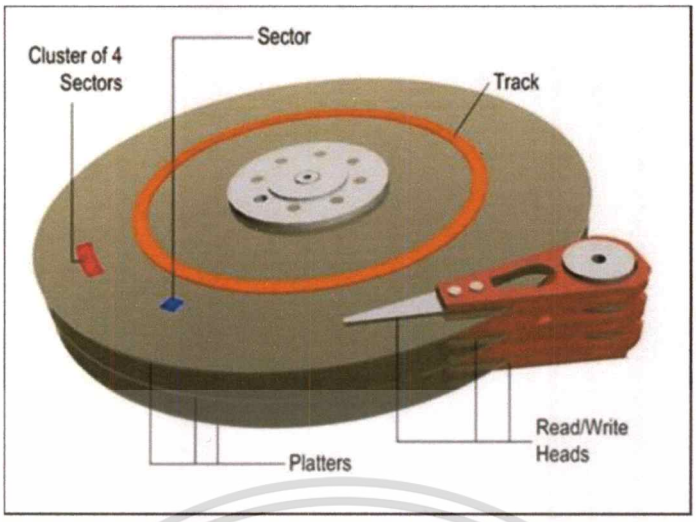

Figure 2.6 A simplified schematic diagram of hard disk drive internals [45]

With the cylinder and head number, the servo system controls the head stack assembly (HSA) to position the selected head to the target track center. The head then waits for the correct sector to begin access the requested data.

Higher HDD capacity is achieved by storing more information in the same physical disks, or increase of the areal density of the disks. Both bit density of tracks and track density of disks must be increased for higher areal density. The former is measured by bits per inch (BPI), and the latter by TPI. Areal density is measured in bits per square inch (BPSI) which is calculated from the multiplication of BPI and TPI.

Areal density is one of the most important factors for HDD performance. It is used to measure how many bits can be packed into each square inch. Increasing TPI is a relatively easier approach to increase the areal density [46], but still a challenging task itself. Historically, it involves cross-discipline technological advances in the magnetic media, actuators design, disk platter material and thickness, servo algorithms, and microprocessors or DSP. The actuator servo system is responsible for maintaining the heads on-track near the center of increasingly narrowed tracks. In typically, higher RPM and more sectors per track result higher sampling rate. The higher sampling rate yields higher HDD internal

performance; however, consume more power, generate more heat, and introduce more self-induced noises. High sampling rate servo system also demands faster DSP speed and reduces the formatting efficiency. The mentioned trade-offs have to be made, Thus, this thesis emphasizes improving the performance of the HDD servo system as the demand of disk drive capacity has continuously been increasing.

HDDs provide an important data-storage medium for computers and other data-processing systems. In most commercial HDDs, rotating disks coated with a thin magnetic layer or recording medium are written with data that are arranged in concentric circles or tracks. Data are read or written with a read/write(R/W) head, which consists of a small horseshoe-shaped electromagnet. Figure 2.7 shows a simple illustration of a typical hard disk servo system with a voice-coil-motor (VCM) actuator.

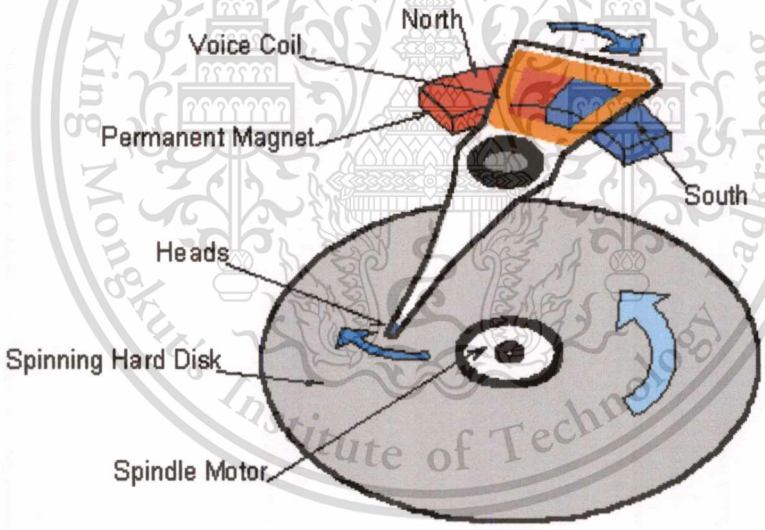

Figure 2.7 VCM actuator servo system in a typical HDD

The two main functions of the R/W head-positioning servomechanism in disk drives are track seeking and track following. Track seeking moves the R/W head from the present track to a specified destination track in minimum time using a bounded control effort. Track following maintains the head as close as possible to the destination track center while information is being read from or written to the disk. Track density is the reciprocal of the

track width. It is suggested that, on a disk surface, tracks should be written as closely spaced as possible so that the usage of the disk surface can be maximized. This means an increase in the track density, which subsequently means a more stringent requirement on the allowable variations of the position of the heads from the true track center. The trend of the hard disk design is towards smaller hard disks with increasingly larger capacities. This implies that the track width has to be smaller, which leads to lower error tolerance in the positioning of the head. The controller for track following has to achieve tighter regulation in the control of the servo mechanism. Typically, the servo system of an HDD can be divided into three stages, i.e. the track-seeking, track-settling and track-following stages (see Figure 2.8 for a detailed illustration).

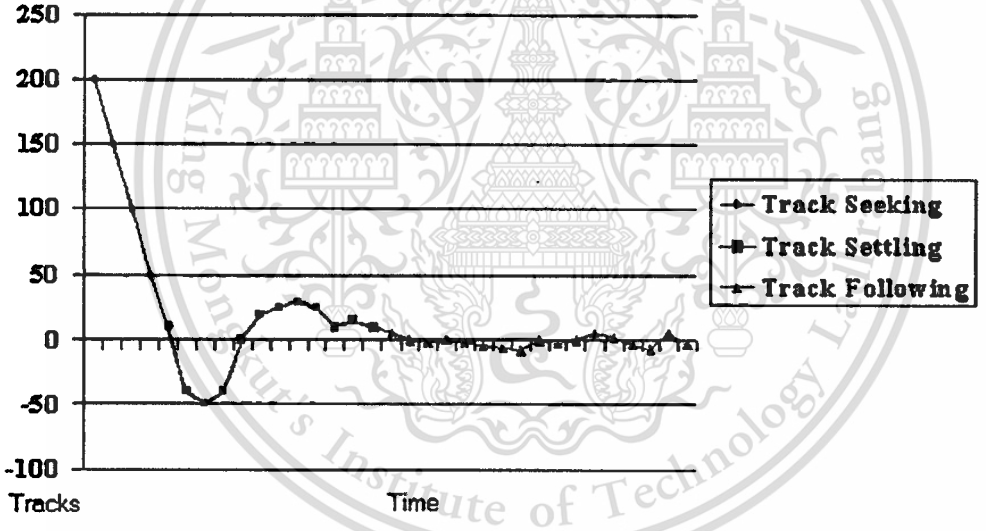

Figure 2.8 Track seeking and following of an HDD servo system [47]

2.3 Issues on Control System Design

For smaller drives with larger capacities, the control system has to achieve tighter regulation in the control of the servomechanism. To read (or write) the data reliably from (or to) the disk, the absolute track-following error with respect to the target track center, which is commonly called TMR - Track Misregistration, must be less than 10% of the track pitch. For example, for a 3.5 HDD with 25 kTPI, the track pitch is about 1 μm and its TMR must be

less than 0.1 μm. Thus, for 70 kTPI, TMR must be less than 0.036 μm. This requires rigorous analysis of the sources of TMR and development of advanced techniques to overcome or eliminate these sources to meet the increasing demand for higher TPI. Figure 2.9 shows a typical disk drive servo channel indicating the various sources of disturbances and errors. Some of the larger components of TMR are due to the following error sources, listed roughly in the order of impact (see, e.g., [34] and references cited therein):

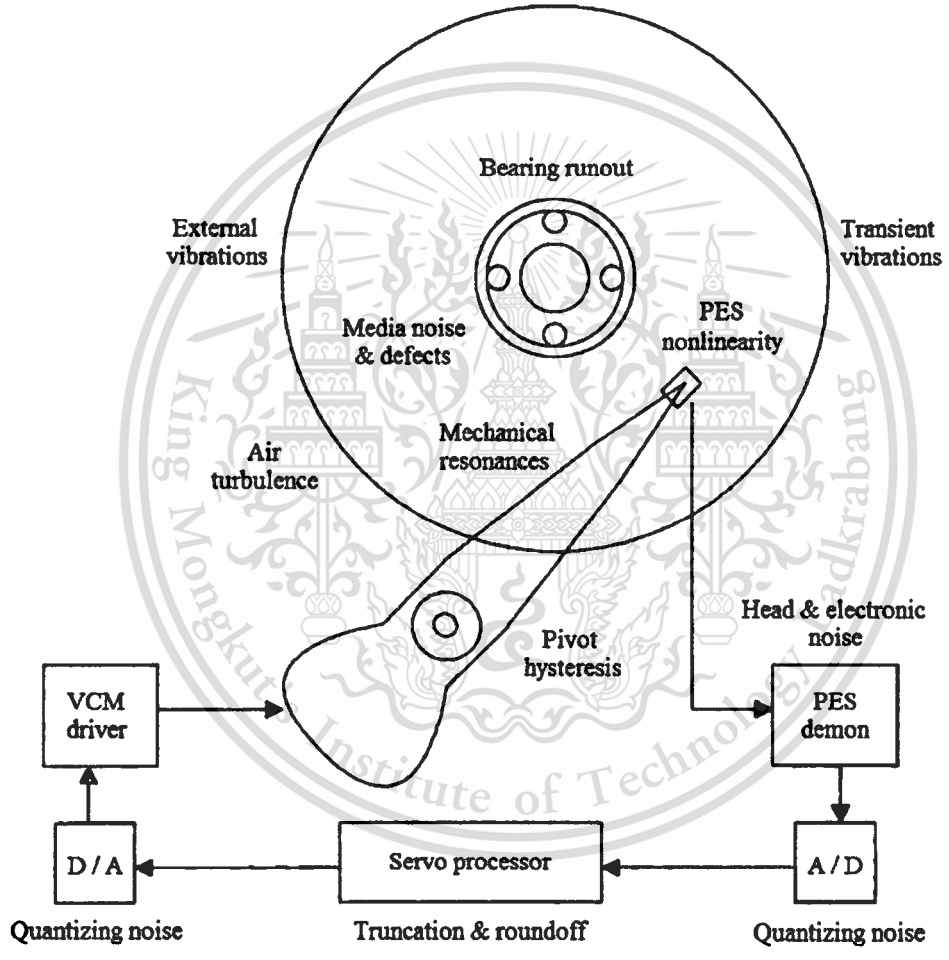

Figure 2.9 Sources of error in an HDD servo system [47]

1. Vibration and external shock definitely present in portable devices;

2. TMR caused by bearing hysteresis effect and poor velocity estimates during track-settling mode;

3. Servo pattern nonlinearities and inaccuracies caused by media, head, and servo writing effects;

4. Mechanical resonance in suspension, actuator disk, and housing;

5. Electronic noise in R/W channel entering the servo demodulator;

6. Non repeatable spindle motor runout caused by bearings;

7. Variations in RRO caused by thermal and other drifts.

A good HDD servo system has no only the desired track-seeking and following performance, but also the robustness to overcome all the above-listed disturbances and uncertainties. The following are robustness issues that one should consider in designing and HDD servo system.

2.3.1 Disturbance Rejection

As mentioned, higher TPI requires a tighter TMR, which is formally defined as three times the position error variance of the true position error signal (PES), i.e. $3\sigma_{pes}$. The sources of disturbances, which are the error sources contributing to $3\sigma_{pes}$, can be classified into three categories: input disturbance, output disturbance and measurement noise. The input disturbance is typically a color noise due to flexure, an electronic bias superimposed with selective energy arising from the natural frequencies of the various mechanical perturbations such as resonances, vibrations and friction. The output disturbance is also a color noise due to spindle rotation and its effects such as runout, windage and media noise. The measurement noise is a typical white noise due to the position-measurement techniques and/or sensors. These disturbances and noise can be modeled as in Figure 2.10.

The objective is to reject the effect of the disturbances and the measurement noise in order to achieve minimum position error variance.

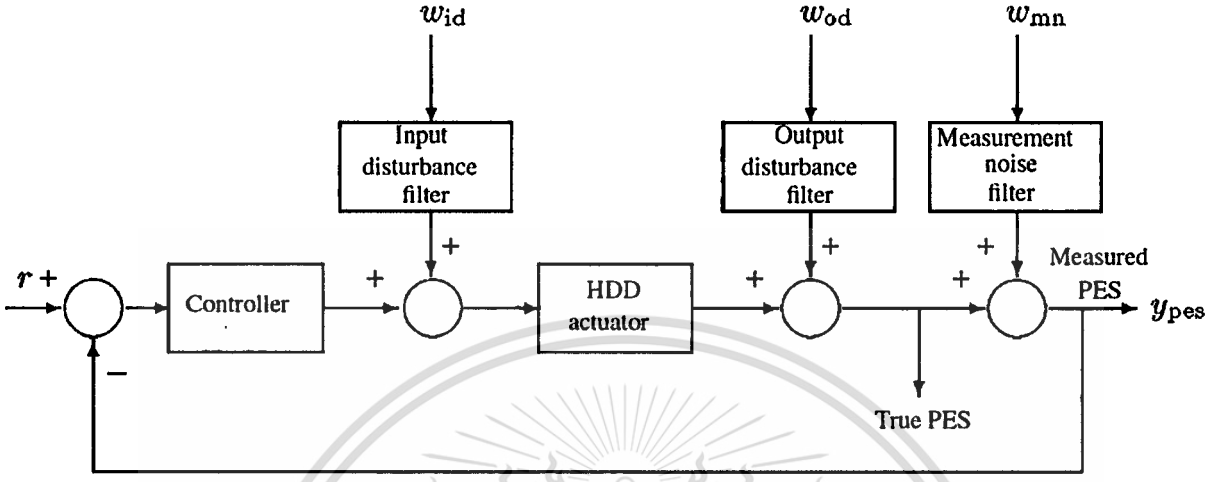

Figure 2.10 Modeling of disturbances in an HDD servo system [47]

2.3.2 Runout Compensation

To understand runout disturbances, The two main functions of HDD servo systems, i.e. track seeking and track following, are recalled. They are usually achieved by two different controllers. The track-seeking controller moves the R/W head to the target track in minimum time. After this, when the control is switched to the track-following controller, it must make the R/W head follow the target track and keep the errors as small as possible. Thus, all HDDs must have a position-measurement mechanism.

The position feedback signals in most HDD servomechanisms are derived through prerecorded position information recorded on one side of a disk surface at the time of manufacture using a servo writer. Ideally, servo tracks are perfect concentric circles. However, in the process of servo writing, the head that writes the signals cannot be performed perfectly due to, e.g., the presence of vibration and NRRO effects, which result in tracks that are not perfect circles. This apparent track motion causes the R/W head to move in an attempt to minimize the position error, which results in positioning of the R/W head

away from the real data track. Such an imperfection is termed a runout. This runout, depending upon its nature, can be classified as repeatable and Non-repeatable.

2.3.2.1 Repeatable Runout

When the sampling frequency is equal to the spindle rotation frequency, or one of its multiples, the runout motion produced by the apparent track is repeated. This repeated runout, which is locked to the spindle rotation in both frequency and phase, is what we call a RRO. Thus, the major source of RROs is the eccentricity of the track. Other sources include the offset of the track center with respect to the spindle center, bearing geometry and wear, and motor geometry [48]. RROs caused by factors other than the eccentricity would cause a large amount of RROs at the rotational frequency of the spindle or its multiples, which is common to all tracks.

2.3.2.2 Non-repeatable Runout

NRROs are a product of disk drive vibration and electrical noise in the measurement channel (see, e.g., [49]). Moreover, the causes of NRRO are spindle-bearing defects, windage-induced disk flutter, electronics noise in the measurement channel, etc., present during servo-track writing. NRROs can be minimized via improved servo writing, use of better bearings, and improved design of electronics. Since RROs are the harmonics of the motor rotational frequency in the frequency domain, an NRRO is the subtraction of the harmonics from the total indicated runout (TIR), which can be defined as the distance difference between the R/W head and the previously written track in an HDD, and hence an NRRO in the time domain can be easily constructed by the inverse Fourier transform of an NRRO in the frequency domain [50]. An NRRO can be taken care of by the servo controller through improved loop bandwidth. However, the increase in servo bandwidth required to reject an NRRO is mainly determined by three factors, i.e. the servo sampling rate, the spectrum of the measurement noise, and the existence of plant resonance modes. The effect of resonance modes and their compensation is discussed in the following section. Recent

research suggests the use of improved mechanical design, with a damped disk substrate and fluid-bearing spindles [51], which imposes less stress on the servo loop, to reject NRROs.

2.3.3 Resonance Compensation

The actuator and HDD structures, of course, are not perfectly rigid and have hundreds of flexible modes. This flexibility gives rise to vibrations, which results in a longer time to settle at the target track and amounts to a significant component of the TMR. In modern disk drives, resonance or vibration modes are the major sources of NRROs. Each resonance mode can be modeled as a second-order transfer function. The VCM actuator transfer function displaying multiple resonance modes can be modeled as [52],

$$G(s) = \frac{k_t}{Js^2} \prod_{i=1}^{n} \frac{w_i^2}{s^2 + 2\zeta_i w_i s + w_i^2} \tag{2.2}$$

where k_t is torque constant, J is inertia, ζ_i and w_i are, respectively, the damping ratio and the natural frequency of the ith resonance mode. For simplicity, the frequency response characteristics with a single resonance mode in actuator dynamics for a typical commercial drive are shown in Figure 2.11, in which the characteristics without resonance mode are shown by dashed lines. There is a significant difference in phase angle of the transfer function with the resonance mode. This tends to cause a loss of gain margin in the compensated loop and hence reduces its stability. Although there are hundreds of such resonances in an actual disk drive, many of the characteristics can be defined by considering only three or four modes, as other modes have an insignificant amplitude or are of too high a frequency to be of interest [50]. Some of the important resonance modes that must be considered in the design of high-density disk drives are the quasirigid body mode, the pivot bearing, the lateral elastic bending. mode, and the vibrations of the individual disk platters.

Currently, the resonances of an HDD head actuator assembly caused by the pivot bearing have become a critical issue, since these resonances have been found to be the major design factor limiting the higher servo control bandwidth [53]. These resonances are

excited during the track-seeking mode, and when the control is transferred to the track-following mode these vibrations result in an increased settling time. Recently, Mah et al. [54] have developed a novel moving-coil head actuator, which is designed deliberately to make sure that the force acting on the VCM is an orthogonal force so that there is no resulting force acting on the pivot bearing, thereby minimizing residual vibrations. The rotational speeds of modern disk drives are progressively increasing, and hence the effect of the vibration of individual disk platters at their natural frequencies is a significant contributing factor to TMR in high-density disk drives.

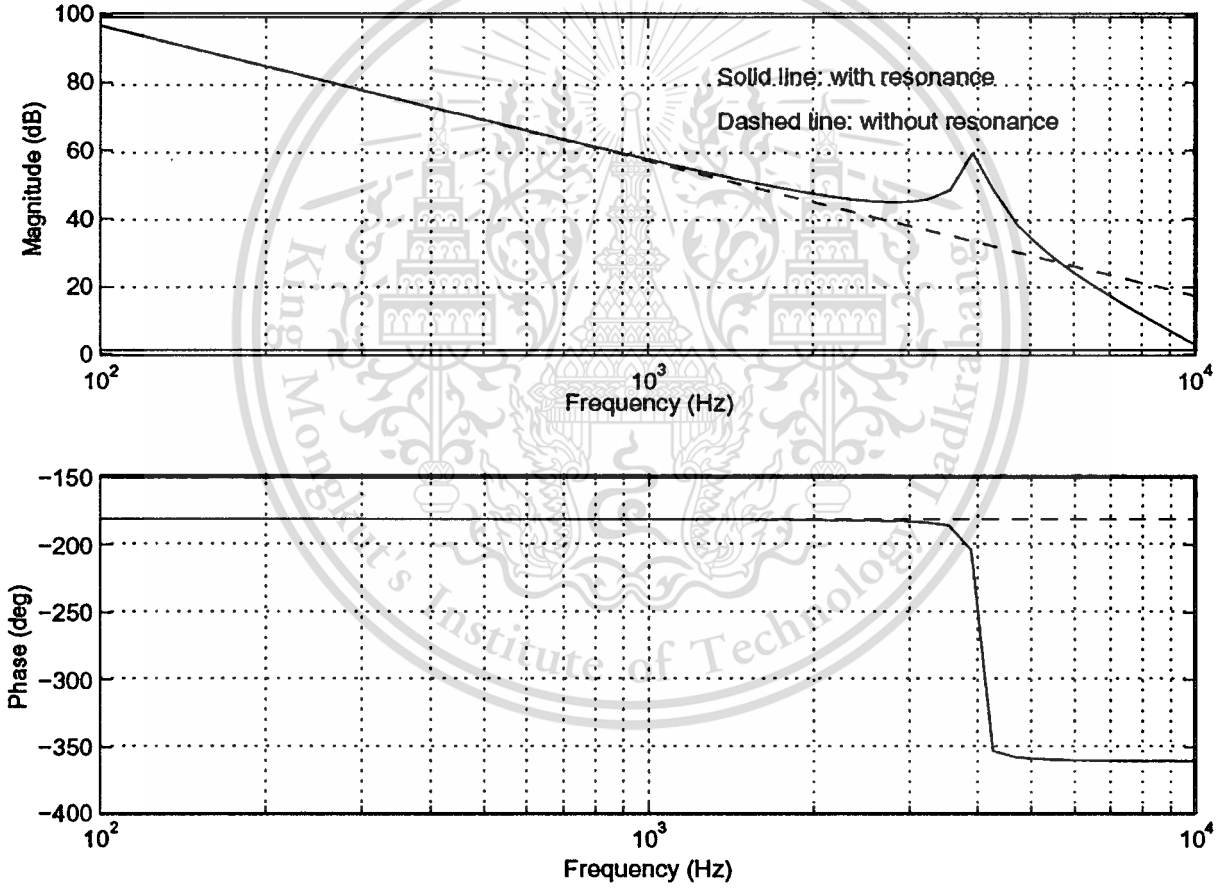

Figure 2.11 The ideal and actual frequency responses of HDD actuators [47]

These resonances are driven primarily by internal windage excitation, and their behavior is dominated by the disk-material properties and geometry, and not by the spindle, encloser, or structural design (see, e.g., [55]). Use of alternate disk substrate materials can control these effects. Structural resonance modes can be compensated by using a notch filter as a precompensator. Since most of all structural resonance modes have lightly damped poles, the idea is to cancel lightly damped poles and place a pair of well-damped poles instead by using a notch filter. Hanselmann and Mortix [56] proposed the use of three notch filters to suppress the plant model resonance modes. These filters are preferred instead of low-pass filters because the sharper the cutoff in the magnitude of the frequency response, the lower the phase introduced in the loop. The transfer function of an analog notch filter is commonly chosen as (see, e.g., [57])

$$G_n(s) = \frac{s^2 + (2\pi f_0)^2}{s^2 + \frac{2\pi f_0}{Q} s + (2\pi f_0)^2} \tag{2.3}$$

Where f_0 is the center frequency and Q is the Q-factor. These notch filters can be realized by using switched capacitance filters. To use with digital control, digital notch filers can be realized using microprocessors or high-speed DSPs. Weaver and Ehrlich [58] proposed the use of multirate filters to eliminate the resonance modes beyond the Nyquist frequency.

As the different objectives in the seeking and the following modes, the control algorithms are often different in the two modes. The overall servo system then involves switches between algorithms. The scheme is referred to as mode switching control (MSC) [59]. There are usually two major issues in the MSC seek controller design: 1) mode switching conditions, and 2) velocity profiles. Track seeking is required to be as fast as possible. Meanwhile, the transition from the seeking to the following mode is also required to be smooth to minimize the residual vibrations [60]. The vibrations may aggravate the head settling, make the effective seek time longer, and cause acoustics problems. A settling mode is often used in between to smooth the transition.

The objective of the track following servo, again, is to maintain the head along the track center precisely. If there were no noise in the servo system, and no servo written-in errors, the perfect tracking would happen and the PES would be consistently zero. Unfortunately, there are many imperfections in reality. Self-induced noises such as air turbulences, disk modes, and sensor noise are random signals by nature; servo written-in errors are deterministic noises. These are the sources contributing to PES consisting of both random and deterministic signals. The positioning accuracy or TMR is measured statistically in terms of the standard deviation σ of the PES. A typical specification is that 3σ be less than 10% of the track width and less than 15% when the drive is subject to vibrations.

Among the trade-offs and several constraints previously stated, fortunately, the robust control systems may successfully be designed by reformulating the design problem as a mixed-sensitivity problem which will be proposed in next chapter.

CHAPTER 3

H_∞ MIXED-SENSITIVITY CONTROL METHOD

3.1 H_∞ Control [61]

All devices are common to have some uncertainties which are difficult to measure and thus to appropriately model, such as the digital implementation and amplifiers delay, or sensor offsets [62]. To deal with these characteristics and get a robust control H_∞ based is proposed. Robust control theory was first developed by Zames in 1979, who considered the minimization of the ∞-norm of the sensitivity function of a single-input-single-output linear feedback system, and it addresses both the performance and stability criterion of a control system. The robust control provides better closed loop control than a PID control.

Let *G(s)* is the open loop transfer function of the plant and *K(s)* is the controller transfer function such that the closed loop system perform robustness and good performance. The controller *K(s)* will be derived keeping three criterions. They are

1. Stability criterion – it states that the roots of the characteristic equation $1+G(s)K(s)=0$ should lie in the left half side of *s* plane.

2. Performance Criterion – it states that the sensitivity $S(s)=\frac{1}{1+G(s)K(s)}$ to be small for all frequencies where disturbances and set point changes is large. Sensitivity is the transfer function between the output and disturbances of a system.

3. Robustness criterion – it demands for stability and performance to be maintained not only for the nominal model but also for a set of neighboring plant models that result from unavoidable presence of modeling errors. Robust H_∞ controllers are developed to provide a highly robust control environment to linear systems.

The detailed design procedure for H_∞ control of linear system is described in works done by Guangzhong Cao, Suxiang Fan, Gang Xu [63], Arredondo and J. Jugo [64], Zdzislaw Gosiewski, Arkadiusz Mystokowski [65].

In general the H_∞ norm of a transfer function, F, is its maximum value over the entire frequency range, and is denoted as

$$\|F\| = \sup_{\omega} \bar{\sigma}(F(j\omega)) \tag{3.1}$$

Where, $\bar{\sigma}$ is the largest singular value of a transfer function. The objective of the synthesis is to design a controller such that the H_∞ norm of the plant transfer function is bounded within limits. Different methods are available for the synthesis of the H_∞ controllers via two transfer function method and three transfer function method. Two transfer function method have less computational complexities and so is considered for H_∞ controller synthesis in this thesis. The robust control problem can be formulated as drawn in Figure 3.1.

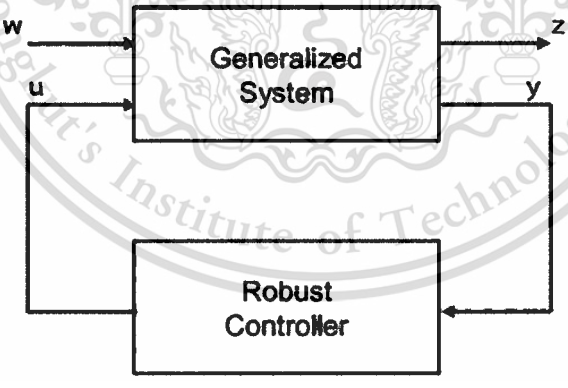

Figure 3.1 Robust Control System

In the traditional H_∞ controller synthesis two transfer functions are used which split a complex control problem into two separate sections, one dealing with stability, the other dealing with performance. The sensitivity function, *S*, and the complementary sensitivity function, *T*, are used in the controller synthesis and given by equations (3.2) and (3.3).

Sensitivity function is the ratio of output to the disturbance of a system and complementary sensitivity function is the ratio of output to input of the system.

$$S = \frac{1}{1+GK} \tag{3.2}$$

$$T = \frac{GK}{1+GK} \tag{3.3}$$

Where '*w*' is the vector of all disturbance signals, '*z*' is the cost signal consisting of all errors. '*v*' is the vector consisting of measurement variables and '*u*' is the vector of all control variables. The controller design problem is then to find a controller *K*, which, based on the information in *v*, generates a control signal *u*, which counteracts the influence of *w* on *z*, thereby minimizing the closed loop norm *w* to *z*. It is done by bounding the values of $\bar{\sigma}(S)$ for performance and $\bar{\sigma}(T)$ for robustness. By minimizing the norm

$$\min_{K} \|N(K)\| \tag{3.4}$$

Where,

$$N = \begin{bmatrix} W_s S \\ W_t S \end{bmatrix} \tag{3.5}$$

Where W_sS and W_tS are the weight functions assigned to the problem by designer. The ultimate aim of the robust control is to reduce the effect of disturbance on output. So sensitivity *S* and the complementary function *T* need to be reduced. For obtaining that it is enough to reduce the magnitude of *S* and *T* . This can be done by making

$$|S(j\omega)| < \frac{1}{W_s(j\omega)} \quad \text{and} \quad |T| < \frac{1}{W_t(j\omega)} \tag{3.6}$$

Where W_s and W_t are the weight function assigned by the designer. W_s is the performance weighting function to limit the magnitude of the sensitivity function and W_t is the robustness weighting function to limit the magnitude of the complementary sensitivity function This

technique called as loop shaping technique which is widely used for selecting the weight functions for the synthesis of the controller and is shown in Figure 3.2 and Figure 3.3.

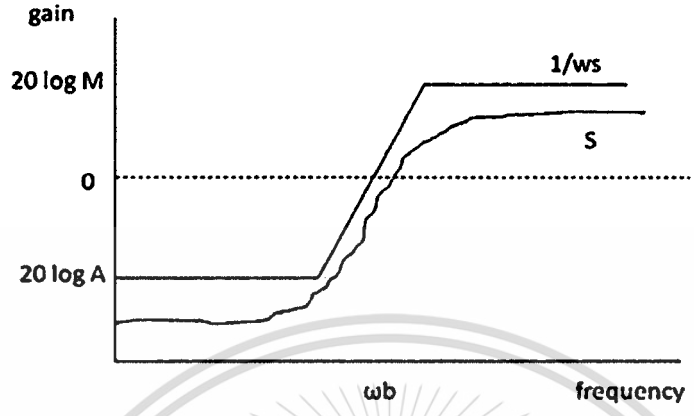

Figure 3.2 Required nature of frequency plots [61]

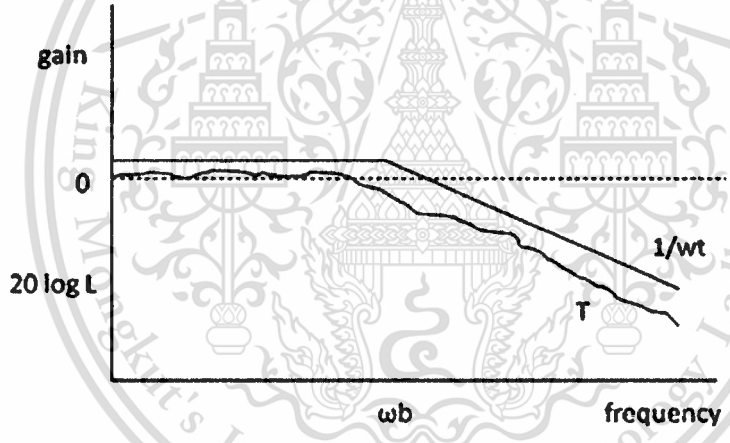

Figure 3.3 Required nature of frequency plots [61]

As mentioned earlier the robust controller is synthesized in order to make the H_∞ norm of the plant to be as low as possible. In order to obtain this condition three weight functions are added to the plant for loop shaping. The weight functions are in fact lead-lag compensators which can shape the frequency response of the system to be in the desired way. Loop shaping which can be implemented in many ways, is done to make the frequency response of the plant with the weight functions to come in the desired manner. In loop shaping, the parameters of the weight functions are changed to make the frequency

response of the whole system to remain within limits. The control synthesis requires the plant transfer function, controller transfer function and the various weight functions to augment together. Thus, an augmented plant model is made as shown in Figure 3.4.

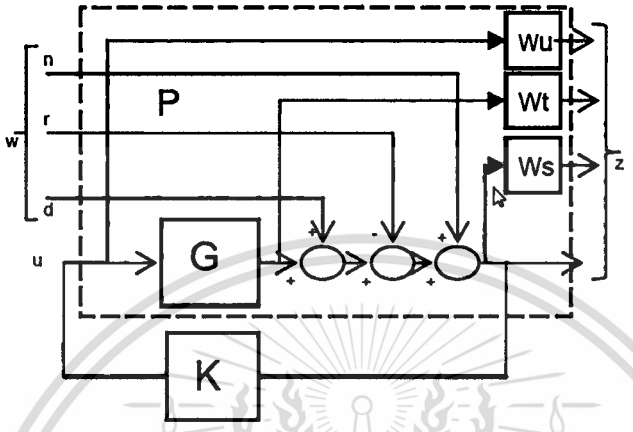

Figure 3.4 Augmented Plant model for the synthesis of H_∞ controller [61]

The normalized frame of the plant is

$$\begin{bmatrix} w_s e \\ w_u u \\ w_t y \\ e \end{bmatrix} = \begin{bmatrix} w_s & -w_s G \\ 0 & w_u \\ 0 & w_t G \\ I & -G \end{bmatrix} \begin{bmatrix} w \\ u \end{bmatrix} \tag{3.7}$$

Where, $U=K*e$. After determining the weights W_s and W_t, the plant can be determined as

$$P = \begin{bmatrix} w_s & -w_s G \\ 0 & w_u \\ 0 & w_t G \\ I & -G \end{bmatrix} = \begin{bmatrix} A & B_1 & B_2 \\ C_1 & D_{11} & D_{12} \\ C_2 & D_{21} & D_{22} \end{bmatrix} \tag{3.8}$$

The equation (3.9) is written as a mixed-sensitivity problem in terms of (3.7) & (3.8) as

$$P = \begin{bmatrix} W_s S \\ W_u R \\ W_t T \end{bmatrix} \tag{3.9}$$

Mixed-sensitivity problem is to find a rational function controller *K(s)* and make the closed loop system stable and satisfy

$$\min\|P\| = \begin{bmatrix} W_s S \\ W_u R \\ W_t T \end{bmatrix} = \gamma \tag{3.10}$$

Where P is the transfer function from *w* to *z* i.e

$$|T_{zw}| = \gamma \tag{3.11}$$

Where $|T_{zw}| = P$ is the cost function. According to the minimum gain theorem, make the H_∞ norm of $|T_{zw}|$ less than unity i.e.,

$$\min\|T_{zw}\| = \min \begin{bmatrix} W_s S \\ W_u R \\ W_t T \end{bmatrix} \leq 1 \tag{3.12}$$

Thus a stabilizing controller *K(s)* is achieved by solving the algebraic riccatti equations minimizing the cost function γ.

As mentioned in the robust control theory the synthesis of the controller requires the selection of two weight functions. The work done by Jiankun Hu, Christian Bohn, H.R. Wu [66] suggests some methods for the election of these weight functions for different plant transfer functions. The works shown in reference [67] also describes some ways for designing robust controller for uncertain plants. In all these design procedure the weighting functions are selected using trial and error method and later the H_∞ controller is synthesized by loop shaping technique. From all these previous works it can be concluded that no straight rules are available for such types of plants till now for the selecting the weight functions. Trial and error method is adopted for loop shaping to find out the controller.

3.2 H_∞ Mixed-Sensitivity Design

In this thesis, track-following controller is designed based on one-degree-of-freedom (1-DOF) using H_∞ mixed-sensitivity loop shaping as controller design technique. The method offers many advantages such as full-matrix controller, incorporation of time-domain specifications via reference model, robustness with known allowable uncertainty bound, design via traditional loop shaping method, and using well established algorithm. The controller produced results comparable to those of the CNF technique but with some advantages mentioned earlier. The objectives of the servo control in term of track-following system are as the followings

1. The actual displacement h tracks a reference r = 1 μm
2. The overshoot is less than 5%
3. The mean of the steady-state error tends to be converged to zero
4. The gain margin and phase margin of the overall design are greater than 6 dB and 30 degrees, respectively
5. The maximum peaks of the sensitivity and complementary sensitivity functions are less than 6 dB
6. The 5% settling time is less than 1 ms

As mentioned, these objectives will become constraints in which the thesis will have to conquer and be able to improve in each parameter.

In automatic control, bandwidth is defined as the frequency at which the gain of the complementary sensitivity function, relating reference *r* to output *y*, declines 3 dB from its steady state. Controller with high bandwidth is preferable for two main reasons. First, the output *y* is able to reproduce the faster reference *r*, resulting in faster output dynamics. Second, the system is able to reject more disturbances that have high frequencies, resulting

in more accurate tracking. The head will be able to move to its desired position and settle down quickly, without overshoot or undershoot beyond the ± 5% window in which the R/W operation can perform including to achieve 5% settling time must less than a millisecond.

The main tool used in this thesis is MATLAB (Matrix Laboratory) which is a numerical computing environment and fourth-generation programming language that developed by MathWorks, to examine and simulate the result. It allows matrix manipulations, plotting of functions and data, implementation of algorithms, creation of user interfaces, and interfacing with programs written in other languages, including C, C++, and Fortran and has the Robust Control Toolbox™ product which is a collection of functions and tools that help us analyze and design SISO control systems with uncertain elements. The LTI system models containing uncertain parameters and uncertain dynamics can be built. This tool will help to analyze SISO system stability margins and worst case performance in the thesis.

MATLAB has a toolbox which includes a selection of control synthesis tools that compute controllers that optimize worst-case performance and identify worst-case parameter values. The toolbox allows to simplify and reduce the order of complex models with model reduction tools that minimize additive and multiplicative error bounds. It provides tools for implementing advanced robust control methods like H_∞, H_2, linear matrix inequalities (LMI), and μ-synthesis robust control.

Studying is started from servo system of the HDD based on single-stage actuator type then formulated to the system plant with 1-DOF then applying the controller box that using H_∞ Mixed-sensitivity technique. Thus, in order to simulate and observe the controller characteristic, MATLAB has a method toolbox which can solve the H_∞ mixed-sensitivity problem in which to synthesis method for robust control loop shaping design.

Syntax [K, CL, GAM, INFO] = mixsyn(G, W_1, W_2, W_3)

Description [K, CL, GAM, INFO] = mixsyn(G, W_1, W_2, W_3) computes a controller K that minimizes the H_∞ norm of the closed-loop transfer function the weighted mixed-sensitivity

$$T_{y_1u_1} = \begin{bmatrix} W_1S \\ W_2R \\ W_3T \end{bmatrix} \tag{3.13}$$

Where *S* and *T* are called the sensitivity and complementary sensitivity respectively and *S*, *R* and *T* are given by

$$\begin{aligned} S &= (I + GK)^{-1} \\ R &= K(I + GK)^{-1} \\ T &= GK(I + GK)^{-1} \end{aligned} \tag{3.14}$$

where γ =GAM. Thus, W_1, W_3 determine the shapes of sensitivity *S* and complementary sensitivity *T*. Typically, W_1 would be chosen to be small inside the desired control bandwidth to achieve good disturbance attenuation (i.e., performance), and W_3 would also be chosen to be small outside the control bandwidth, which helps to ensure good stability margin (i.e., robustness). For dimensional compatibility, each of the three weights W_1, W_2 and W_3 must be either empty, scalar (SISO) or have respective input dimensions N_Y, N_U, and N_Y where *G* is N_Y-by-N_U. If one of the weights is not needed, It may be simply assigned as an empty matrix []; e.g., *P* = AUGW(*G*, W_1, [], W_3) is SYS but without the second row (without the row containing W_2).

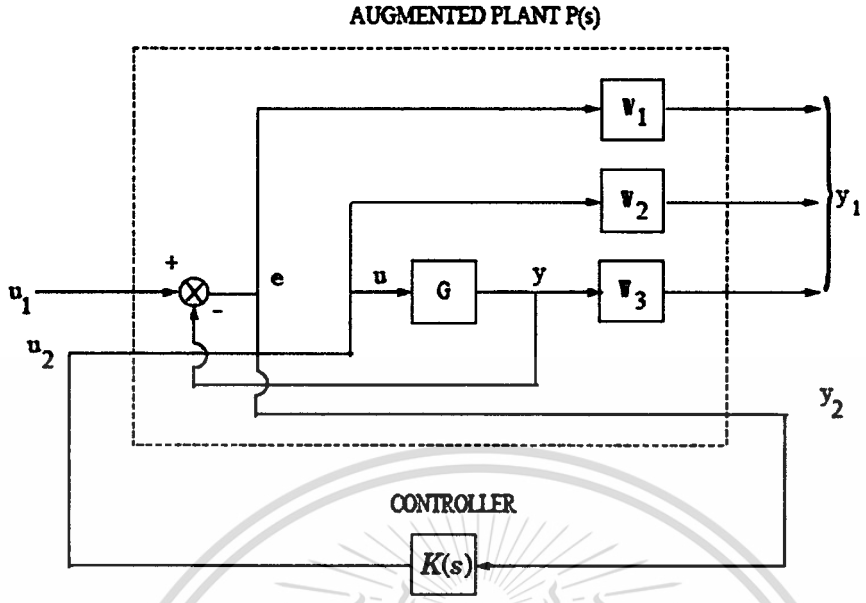

Figure 3.5 Closed-loop transfer function for mixed-sensitivity [68]

The returned values of S, R, and T satisfy the following loop shaping inequalities:

$$\begin{aligned} \bar{\sigma}(S(j\omega)) &\le \gamma \underline{\sigma}(W_1^{-1}(j\omega)) \\ \bar{\sigma}(R(j\omega)) &\le \gamma \underline{\sigma}(W_2^{-1}(j\omega)) \\ \bar{\sigma}(T(j\omega)) &\le \gamma \underline{\sigma}(W_3^{-1}(j\omega)) \end{aligned} \tag{3.15}$$

CHAPTER 4

SIMULATION

4.1 Single Stage Actuator Model

Chen et al. (2006) identified a transfer function model of a Maxtor 51536U3 drive and designed several track-following control systems. This control system was designed based on their model and compared the results with their work. For completeness, their model is presented in this section.

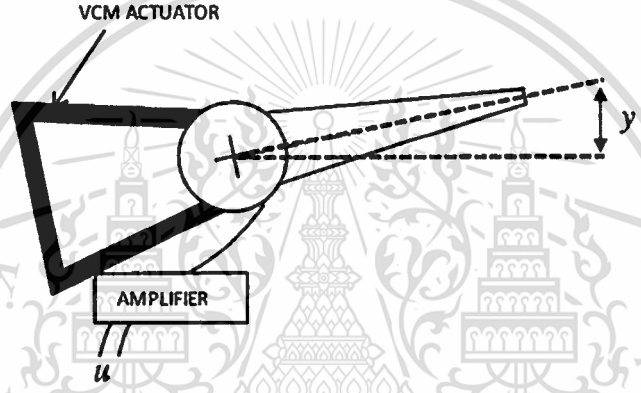

Figure 4.1 Diagram of Single-Stage Actuator

Consider block diagram in Figure 4.1. *u* are voltage inputs and *y* are linear displacements in micrometers of the VCM actuator. A frequency-varying sine wave was inputted as *u*. The resulting output *y* was recorded, and both were sent to a dynamic signal analyser (model SRS 785.) A Bode plot was generated, and a transfer function, consisting of a low-frequency nominal model and four high frequency resonance modes, were obtained as

$$G(s) = \frac{y(s)}{u(s)} = \frac{6.4013 \times 10^7}{s^2} \prod_{i=1}^{4} G_{r,i}(s) \tag{4.1}$$

Several constraints and requirements are as the following. First, $|u| \leq 3$. Second, the overshoot and undershoot are less than 5%, so the head can start R/W operations immediately. Third, the gain and phase margin are greater than 6 dB and 30°. Fourth, the

sensitivity and complementary sensitivity functions have peaks less than 6 dB. Fifth, the sampling frequency is 20 kHz. The Equation (4.1) can be expanded as

$$
\begin{aligned}
G_{r,1}(s) &= \frac{0.912s^2 + 457.4s + 1.433\times10^8}{s^2 + 359.2s + 1.433\times10^8}, \\
G_{r,2}(s) &= \frac{0.7586s^2 + 962.2s + 2.491\times10^8}{s^2 + 789.1s + 2.491\times10^8}, \\
G_{r,3}(s) &= \frac{9.917\times10^8}{s^2 + 1575s + 9.917\times10^8}, \\
G_{r,4}(s) &= \frac{2.731\times10^9}{s^2 + 2613s + 2.731\times10^9},
\end{aligned}
\tag{4.2}
$$

Resonant frequencies may also change due to many other factors, for example, changes in operating conditions, age of the components etc. To address this issue, a notch filter that can accommodate such variations in the resonant frequencies should be used. Notch filter or band-reject filter was used in series with the VCM actuator which can solve the problem of residual vibration. It inhibits the band of frequencies around the resonant frequency from reaching the R/W head. Notch filters not only attenuates the frequencies around the frequency of resonance but also modifies the phase of the open loop transfer function The notch filter for the VCM actuator was given by

$$
\begin{aligned}
G_{notch}(s) = &\left(\frac{s^2 + 238.8s + 1.425\times10^8}{s^2 + 2388s + 1.425\times10^8}\right) \\
&\times\left(\frac{s^2 + 314.2s + 2.467\times10^8}{s^2 + 3142s + 2.467\times10^8}\right) \\
&\times\left(\frac{s^2 + 628.3s + 9.87\times10^8}{s^2 + 12570s + 9.87\times10^8}\right)
\end{aligned}
\tag{4.3}
$$

Whose frequency response is given in Figure 4.2 The overall response of the plant together with the notch filter is given in Figure 4.3. It can be obviously noticed that the effect of the first two resonance modes are able to be reduced by the filter.

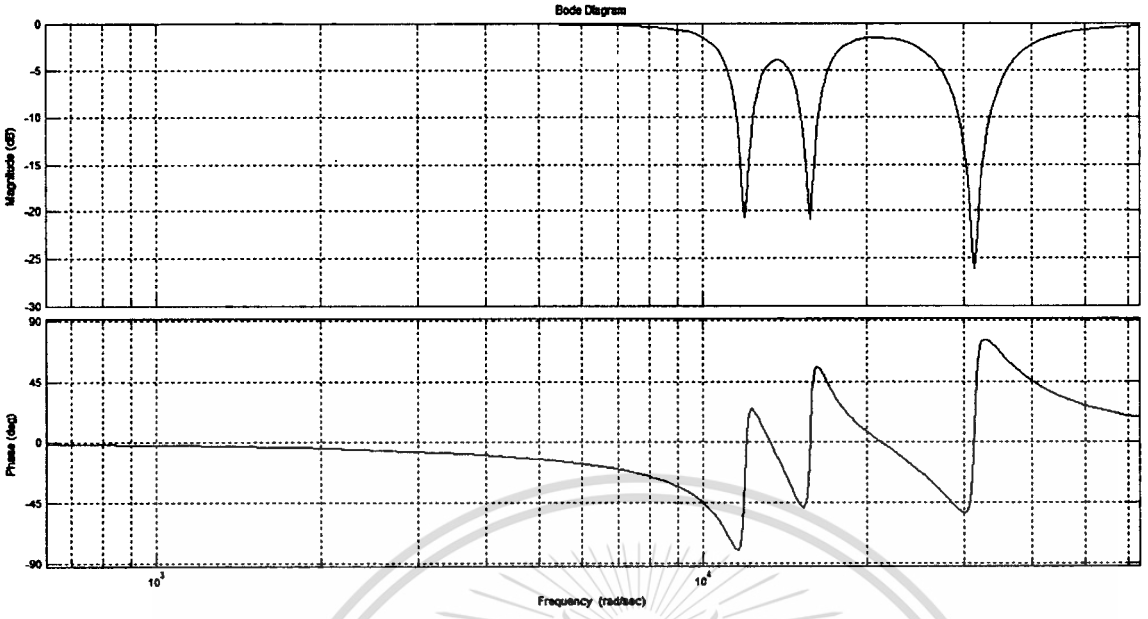

Figure 4.2 Frequency responses of the notch filter

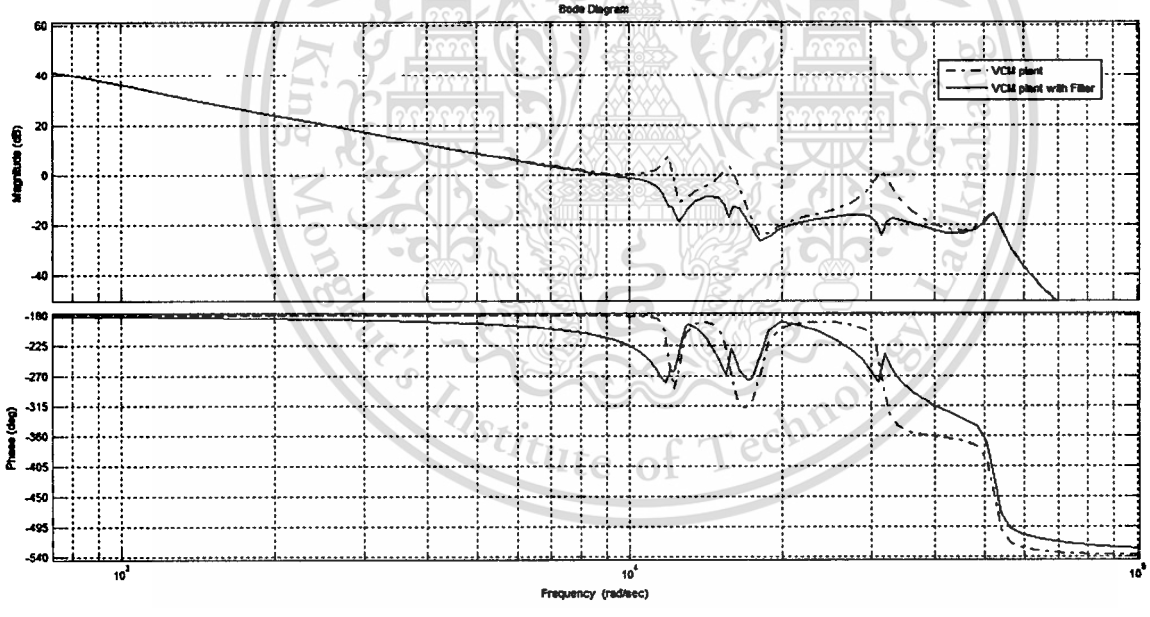

Figure 4.3 Frequency responses of the VCM plant with the notch filter

Figure 4.4 contains the block diagram of overall control system. The controller K represents an optimal control system, which was designed using H_∞ mixed-sensitivity method presented next.

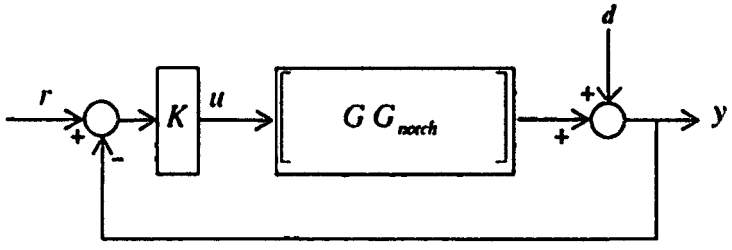

Figure 4.4 Block diagram of overall control system.

4.2 H_∞ Mixed-sensitivity Design Methodology

The feedback controller design problem can be formulated as an H_∞ optimization problem, which can be posed under the general configuration shown in Figure 4.5 [69]. In this figure, *P(s)* is the generalized plant, *K(s)* is the controller, *u* are the control input signals, *v* are the measured variables, ω are the exogenous signals and *z* are the error variables.

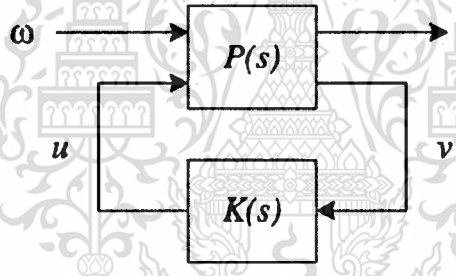

Figure 4.5 Block diagram of control problem

The optimal H_∞ control problem with this configuration consists of computing a controller such that $\|T_{zw}\| \leq 1$ which yields the ratio γ between the energy of the error vector *z* and the energy of the exogenous signals vector ω is minimized which it should be less than unity. This optimal problem is not solved yet, but a solution exists for the suboptimal problem (see [70] for the continuous time domain case and [71] in case of discrete time domain). Whereby, the value of the energy ratio γ is decreased as much as possible by means of an iteration process. This is the synthesis process which has been implemented in various well-known software packages such as [72] or [73].

A configuration for building up the generalized plant is the *S/T* mixed-sensitivity problem (see, for example, [74]), which is exposed in Figure 4.6 [69]. In this case, the expression of the resulting closed loop transfer function $T_{z\omega}(s)$ is as follows:

$$T_{z\omega}(s)=\begin{bmatrix} W_S(s)S_O(s) \\ W_T(s)T_O(s) \end{bmatrix} \tag{4.5}$$

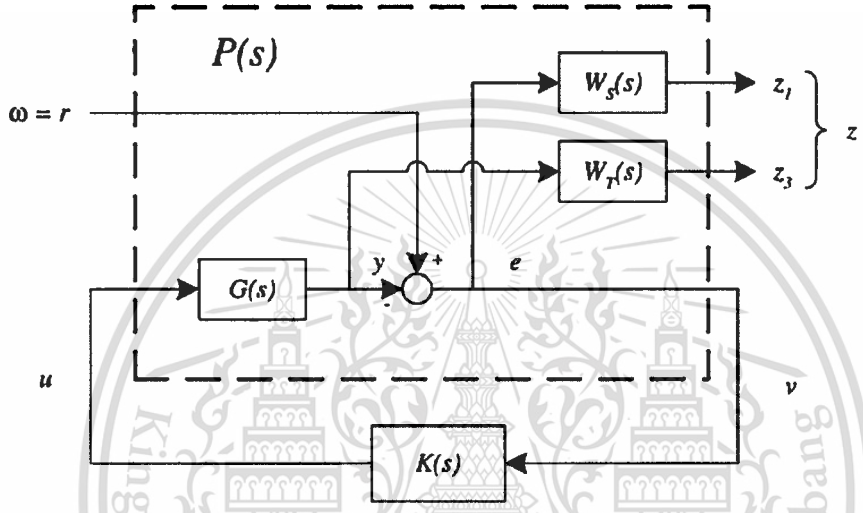

Figure 4.6 S/T mixed-sensitivity configuration

where $S_o(s)$ is the output sensitivity transfer matrix and $T_o(s)$ is the output complementary sensitivity transfer matrix:

$$\begin{aligned} S_O(s) &= (I+G(s)K(s))^{-1} \\ T_O(s) &= G(s)K(s)(I+G(s)K(s))^{-1} \end{aligned} \tag{4.6}$$

The terms $W_S(s)$ and $W_T(s)$ constitute their respective weighting matrices, which allow the range of frequencies of main importance for the corresponding closed-loop transfer matrix to be specified. As it is known, shaping $T_o(s)$ is desirable for tracking problems, noise attenuation and for robust stability with respect to multiplicative output uncertainties. On the other hand, since $S_o(s)$ relates the error signals with references and disturbances [75], shaping the sensitivity function will allow the performance (in terms of command tracking and disturbance attenuation) of the system to be controlled.

Therefore, since the controller is obtained from the generalized plant, the synthesis problem with this configuration is reduced to the design of a nominal model *G(s)* and some appropriate weighting matrices which will impose the control specifications. Once these designs have been carried out, the generalized plant can be built up, and consequently the controller can be computed by means of a synthesis algorithm implemented in a computer.

In this section, the weight functions are given by using an empirical formula to determine the performance and robustness weight for a general H_∞ control problem is suggested by Skogestad and the work in [74], and is given in Equations (4.7).

$$W_S = \frac{s/M + w_b}{s + w_b A}, W_T = \frac{Ls + 1}{2(0.5Ls + 1)} \tag{4.7}$$

Where W_S is the performance weighting function, 'M' is the gain for high frequency disturbances, 'w_b' is the cut off frequency, 'A' is the gain for low frequency control signal and 'L' is a constant. 'w_b' is the frequency which differentiates the high frequency disturbance signal and the low frequency control signal. The plots, Figures 3.2 and 3.3 show the nature of sensitivity function S and its boundary $1/W_S(s)$ including complementary sensitivity function T and its boundary $1/W_T(s)$ to be satisfied for the synthesis of H_∞ controller which can be done by closely shaping the $1/W_S(s)$ and $1/W_T(s)$ plot. This loop shaping technique is adjusting the various parameters of the weight functions to be closed to the curves in order to make a robust H_∞ controller.

Using a function in the MATLAB control toolbox named "*mixsyn*" to synthesize an optimized controller which corresponds to the actuator plant. The various parameters given in Equation (4.7) are chosen, i.e., M=2, W_b=1000π, A=1/100 and L=4x10^{-4}. Thus, the plant, sensitivity weight and its complementary weight function are determined from that empirical formula to input for this synthesis as follows:

$$W_S = \frac{0.5s + 3142}{s + 31.42}, W_T = \frac{0.735s + 1571}{0.01s + 3142} \tag{4.8}$$

The validity of the proposed design methodology of H_∞ controllers is implemented in track-following of HDD actuator, which constitutes a typical example of HDD. The simulation results of the H_∞ design are presented and compared to the PID - Proportional-Integral-Derivative, RPT – Robust & Perfect Tracking and CNF – Composite Nonlinear Feedback control algorithm.

4.2.1 Performance Analysis

The simulation result of the closed-loop responses for the control system is shown in Figures 4.5 and 4.6 [47]. Ziegler-Nichols tuning is used to design the PID controller which is given as follows,

$$K_p = \frac{3K_u}{5},\ T_i = \frac{\pi}{\omega_u},\ K_p = \frac{\pi}{\omega_u} \tag{4.9}$$

Where K_u is a simple proportional gain that is increased until the continuous oscillations in its step response can be observed, i.e. the system becomes marginally stable. Then the ω_u can be obtained as the corresponding oscillating frequency.

It is noted that the PID control generates large overshoots as shown in Figure 4., while the system with other methods including H_∞ control have very little overshoot. The 5% settling time, which is commonly used in the HDD research community, is summarized in Table 4.1 which is modified from [47]. Clearly, the H_∞ control gives better performance than other methods except CNF.

Table 4.1 Performances of the track-following controllers

	Settling time (ms)			
	PID	RPT	H_∞	CNF
Simulation	3.10	0.95	0.86	0.80

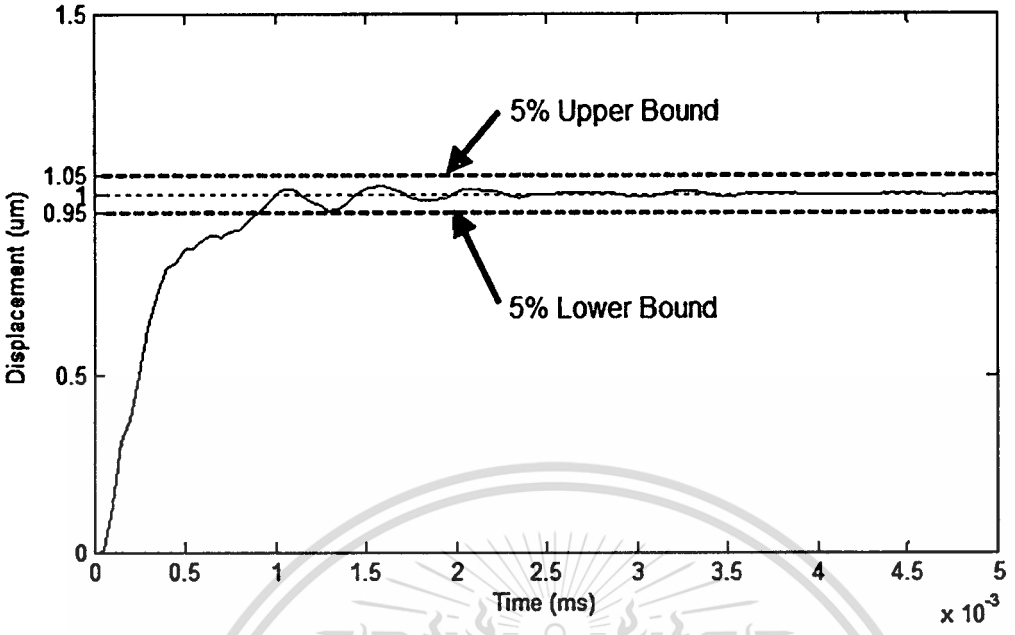

Figure 4.7 Output step response of H_∞

4.2.2 Stability and Robustness Analysis

Stability analysis is done to ensure the stability of track-following operation using the H_∞ method. The bode plot of the closed loop sensitivity function of the robust controlled actuator is shown in Figure 4.7. The plot shows that the system is stable for a wide range of frequencies of the actuator's operating frequency ranges.

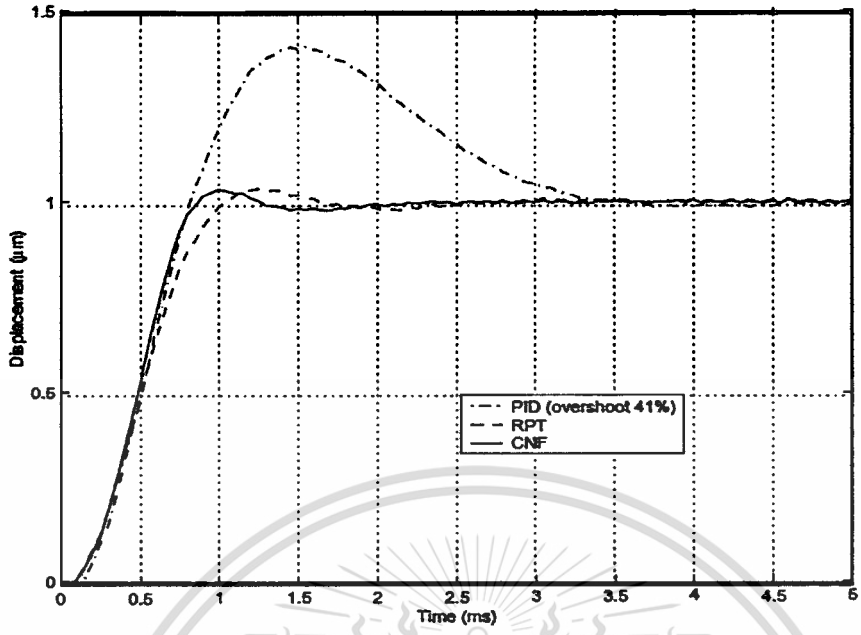

Figure 4.8 Output responses of other control methods

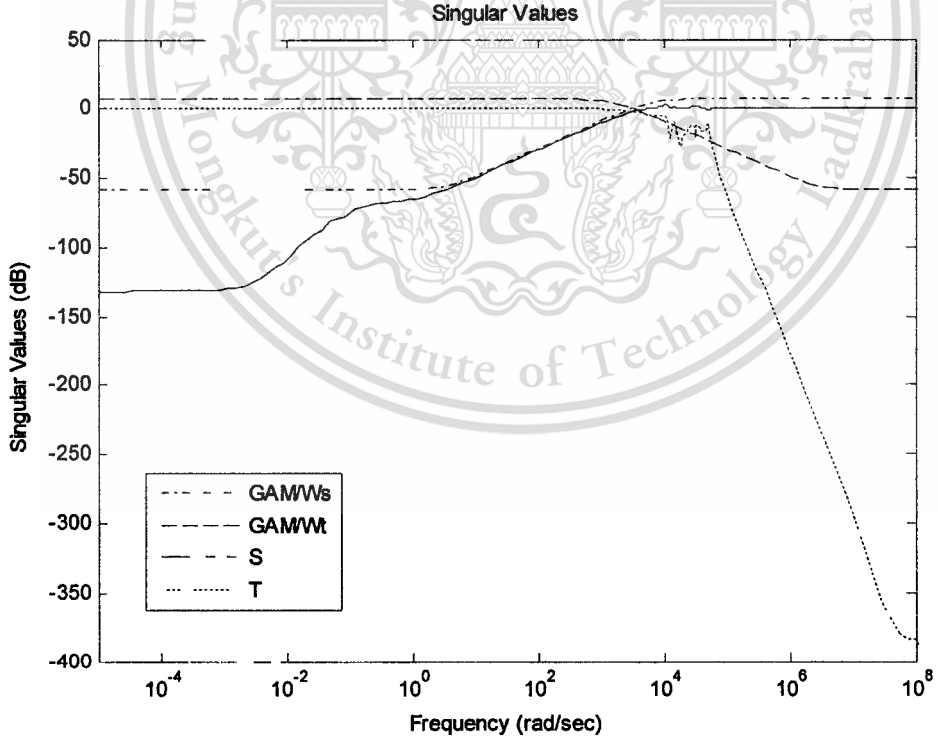

Figure 4.9 Singular values of H_∞

The figure shows the singular values of sensitivity function, complementary sensitivity function with H_∞ control. The singular values of sensitivity function and complementary sensitivity function of actuator plant controlled under H_∞ method lies below the zero gain for range of operating frequencies. The sensitivity '*S*' and its complementary '*T*' are under their boundary '*GAM/Ws*' and '*GAM/Wt*' within the range of operating frequencies from 10^0 to 10^4 rad/sec, respectively. Furthermore, Peak of both sensitivity and complementary functions meet the design specification given in the section 4.1 with values are less than 6 dB.

4.3 H_∞ Mixed-sensitivity Design Benchmark

In order to make it clear in the actual implementation, the synthesized controller *K* designed from the H_∞ mixed-sensitivity technique should have an excellent benchmark to illustrate how well it could be in real situation.

The closed-loop diagram of the actuator shown in Figure 4.4 is recalled with a measurement noise added in as shown in Figure 4.10.

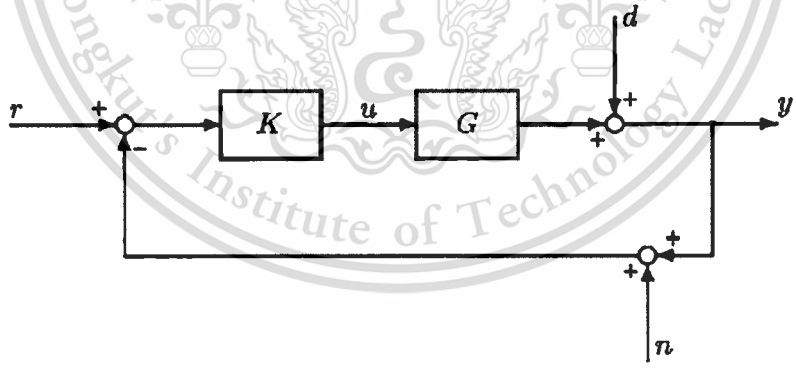

Figure 4.10 Closed-loop diagram of the dynamical model of the HDD VCM actuator

where the control input *u* is limited within ±3 V and d is an unknown input disturbance with $|d| \le 3$ mV. For simulation purpose and simplicity, the unknown disturbance is assumed to be $d = -3$ mV. The measurement output available for control, i.e. *y* (in μm), is the measured displacement of the VCM R/W head and given by

$$y(s) = T(s)r(s) + S(s)d(s) - T(s)n(s)] \tag{4.8}$$

and the control effort, i.e. *u* (in V), is the input signal and is given by

$$u(s) = K(s)S(s)[r(s) - n(s) - d(s)] \tag{4.9}$$

In Figure 4.11, the notch filter stated in Equation (4.3) is included in *G*. The output disturbance (in μm), which is mainly the repeatable runouts, is given by

$$d = 0.1\sin(110\pi t) + 0.05\sin(220\pi t) + 0.02\sin(440\pi t) + 0.01\sin(880\pi t) \tag{4.10}$$

and the measurement noise is assumed to be a zero-mean Gaussian white noise with a variance $\sigma_n^2 = 9\times10^{-6}$ (μm)^2.

When the problem of controller design is applied to the VCM actuator system, the result of the closed-loop system is asymptotically stable and the actual displacement of the actuator, i.e. y, tracks a reference *r* = 1 μm.

The simulation results can be obtained obviously that all the design requirements stated in section 3.2 have been achieved. In particular, the maximum values of the sensitivity and complementary sensitivity functions are less than 5 dB. The overall control system can still produce a satisfactory result and satisfy all the design specifications when agitated by disturbances. Figure 4.12 shows the control effort indicating its efficacy of disturbance rejection and reference tracking which also sustained in Figure 4.13. The first subplot in Figure 4.13 shows the efficacy of output response of overall system *y(s)* including noise and disturbance attenuation. The second subplot shows performance of reference tracking *T(s)r(s)*. The third and fourth plots show performance of disturbance rejection *S(s)d(s)* and noise attenuation *T(s)n(s)*, respectively.

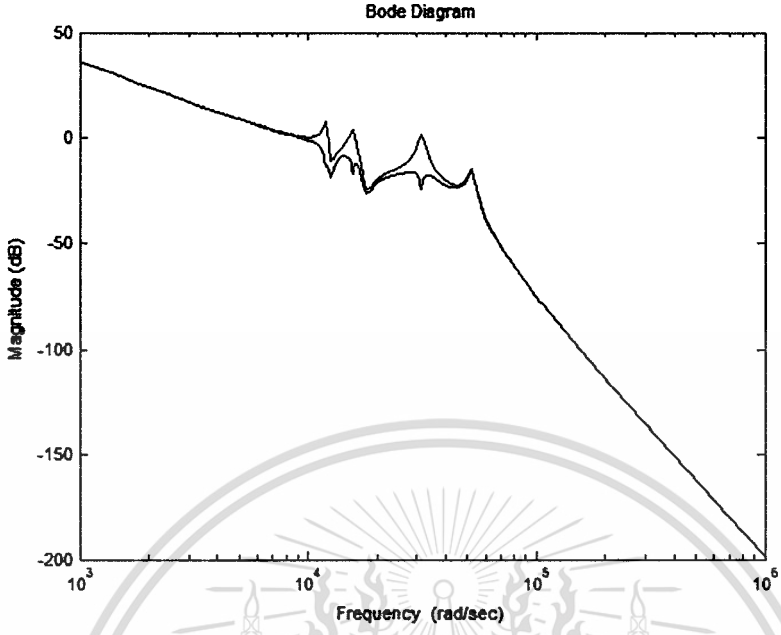

Figure 4.11 Bode plot of the plant with (green) and without (blue) notch filter

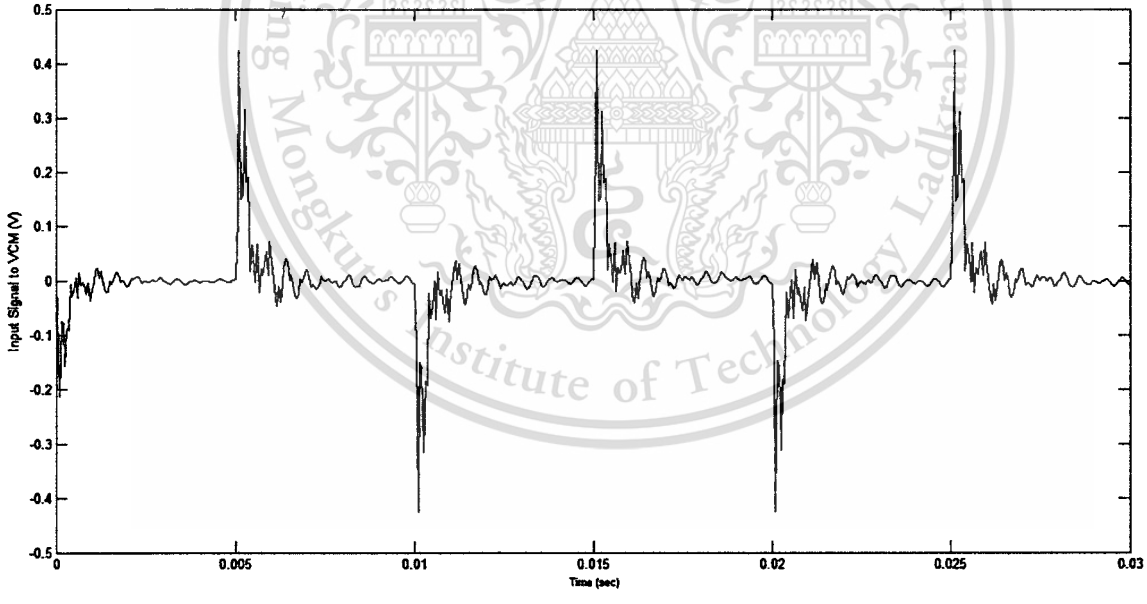

Figure 4.12 Control effort from input u

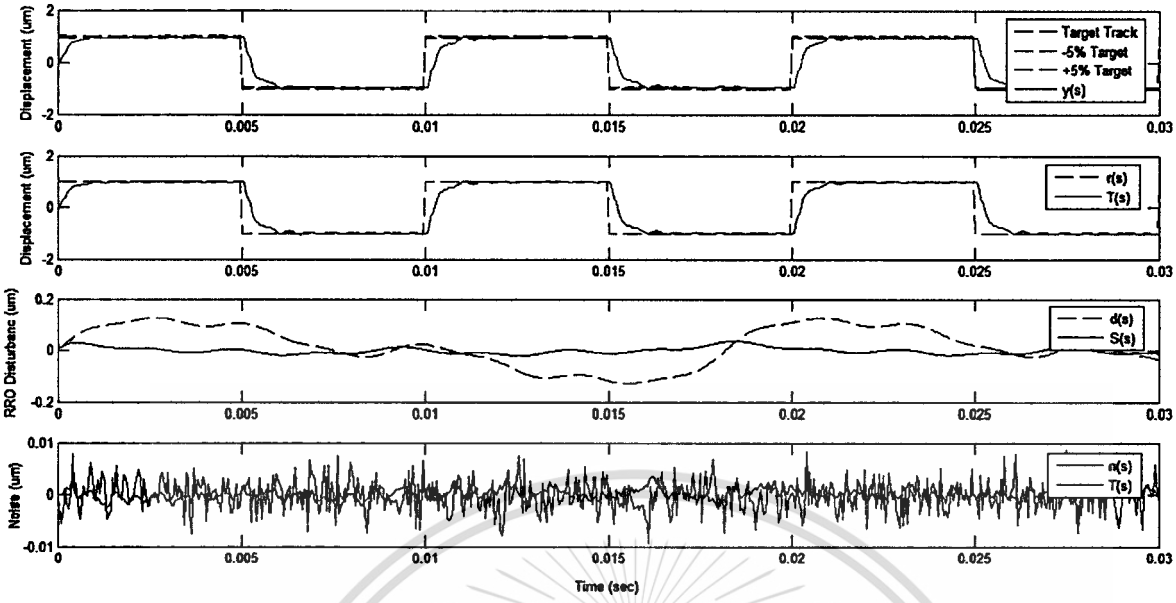

Figure 4.13 Tracking and disturbance rejection

CHAPTER 5

CONCLUSION

H_∞ methods are widely used in control theory to synthesize controllers achieving stabilization with guaranteed performance. To use H_∞ methods, a control designer expresses the control problem as a mathematical optimization problem and then finds the controller that solves this optimization. H_∞ optimization introduced a control approach called "mixed-sensitivity" which has the advantage over classical control techniques in that it is readily applicable to problems involving to achieve design targets compatible with good performance and robustness.

In this thesis, the H_∞ mixed-sensitivity control is proposed to be applied track-following control of a HDD single actuator. In H_∞ control synthesis using loop shaping technique, two weight functions are to be designed to shape the closed loop characteristics of the system. The selection of these two weight functions are normally a trial and error initialized by an empirical formula including the detailed analysis of the system requirements. A detailed analysis of the developed H_∞ controller for stability, performance and robustness has been made for actuator including value of the energy ratio γ is 0.9844 which meets the minimum gain theorem that aims to minimize the H_∞ norm to be less than unity. The results show that the H_∞ controller could stabilize the track-following system with good performance and robustness within the design specification. The step response shown in Figure 4.7 indicates the H_∞ control proposed in this thesis could bring the system back to its equilibrium point in the least possible time second only to the CNF method.

Nonetheless, disadvantages of H_∞ techniques include the level of mathematical understanding needed to apply them successfully and the need for a reasonably good model of the system to be controlled. It is important to keep in mind that the resulting controller is only optimal with respect to the prescribed cost function and does not necessarily represent the best controller in terms of the usual performance measures used

to evaluate controllers such as settling time, energy expended, etc. Also, non-linear constraints such as saturation are generally not well-handled.

REFERENCES

[1] K. J. Astrom et al., **"Zeros of sampled systems,"** in Automatica (Journal of IFAC), 1984, pp. 31-38.

[2] B. Hurst, **"Keeping track: how to test a 20 gb/sqin drive,"** in Data Storage, 1999.

[3] M. Tomizuka et al., **"Disturbance rejection through an external model,"** in Journal of Dynamics Measurement and Control, 1990, pp. 559-564.

[4] M. Tomizuka, **"Model based prediction, preview and robust controls in motion control systems,"** Proc. IEEE 4th Advanced Motion Control, Japan, 1996, pp. 197-202.

[5] M. Tomizuka, **"On the design of digital tracking controllers,"** in Journal of Dynamic Systems, Measurement and Control, vol. 115, 1993, pp. 412-418.

[6] M. Tomizuka, **"Zero-phase error tracking controller for digital control,"** in ASME Journal of Dynamics, Measurement and Control, vol. 109, 1987, pp. 65-68.

[7] K.K. Chew, **"Control system challenges to high track density magnetic disk storage,"** IEEE Trans. Magn., vol.32, 1996.

[8] KK. Chew, **"Constrained linearization of embedded position error signals (PES),"** Proc. 24th Annual Conference of the IEEE Industrial Electronics Society, Aachen, Germany, 1998, pp. 1477-1480.

[9] R. Ehrich and D. Curran, **"Major HDD TMR sources and projected scaling with TPI,"** IEEE Trans. Magn., vol. 32, pp. 1799-1804, 1996.

[10] R. Ehrich, **"TPI growth is key to delaying superparamagnetism's arrival,"** in Data Storage, vol. 6, 1999.

[11] M. White and WM. Lu, **"Hard disk drive bandwidth limitations due to sampling frequency and computational delay,"** Proc. 1999 IEEE/ASME International Conference on Advanced Intelligent Mechatronics, GA, 1999, pp. 120-125.

[12] J.S. McAllister, **"The effect of disk patter resonances on track misregistration in 3.5 inch disk drives,"** IEEE Trans. Magn., vol.32, 1996.

REFERENCES (CONT.)

[13] C. D'Angelo III and C.D. Mote Jr., **"Natural frequencies of a thin disk, clamped by thick collars with friction at the contacting surfaces, spinning at high rotation speed," in** Journal of Sound and Vibration, vol. 168, 1993, pp. 1-14.

[14] D. Abramovitch et al., **"Decomposition of baseline noise sources in hard disk position error signals using the pes pareto method,"** Proc. American Control Conf., NM, 1997, pp. 2901-2905.

[15] D. Abramovitch et al., **"Measurement for the PES pareto method of identifying contributors to disk drive servo systems errors,"** Proc. American Control Conf., NM, 1997, pp. 2896-2900.

[16] D. Abramovitch et al., **"The pes pareto method: uncovering the strata of position error signals in disk drives,"** Proc. American Control Conf., NM, 1997, pp. 2888-2895.

[17] D. Abramovitch et al., **"An overview of the PES pareto method for decomposing baseline noise sources in hard disk position error signals,"** IEEE Trans. Magn., vol.34, pp. 17-23, 1998.

[18] H.T. Ho, **"Noise impact on servo TMR,"** Proc. American Control Conf., NM, 1997, pp. 2906-2909.

[19] H.S. Lee and L. Guo, **"Servo performance prediction for high capacity disk drives,"** Proc. American Control Conf., 1998.

[20] J. Li and T.C. Tsao, **"Rejection of repeatable and non-repeatable disturbances for disk drive actuators,"** Proc. American Control Conf., San Diego, CA, 1999, pp. 3615-3619.

[21] C. Kempf et al., **"Comparison of four discrete time repetitive control algorithms,"** IEEE Control. Syst. Mag., vol. 13, no. 6, pp. 48-54, 1993.

REFERENCES (CONT.)

[22] K.K. Chew and M.Tomizuka, **"Digital control of repetitive errors in disk drive systems,"** IEEE Control Syst. Technol., pp. 16-20, 1990.

[23] C. Smith and M. Tomizuka, **"Shock rejection for repetitive control using a disturbance observer,"** Proc. 35th IEEE Conf. on Decision and Control, Kobe, Japan, 1996, pp. 2503-2504.

[24] J. Ishikawa and M. Tomizuka, **"Pivot friction compensation using an accelerometer and a disturbance observer for hard diak drives,"** in ASME International Mechanical Engineering Congress and Exposition, 1997.

[25] M.T. White and M. Tomizuka, **"Increased disturbance rejection in magnetic disk drives by acceleration feed-forward control and parameter adaptation,"** Control Engineering Practice, vol. 5, no. 6, 1997, pp. 741-751.

[26] M.T. White and M. Tomizuka, **"Increased disturbance rejection in magnetic disk drives by acceleration feed-forward control,"** Proc. 13th World Congress, International Federation of Automatic Control, San Francisco, CA, 1996, pp. 489-494.

[27] B. Amstrong-Helouvry et al., **"A survey of models, analysis tools and compensation methods for the control of machines with friction," in** Automatica, vol. 30, 1994, pp. 1083-1138.

[28] H. S. Chang et al., **"Modeling of pivot friction using relay function and estimation of its frictional parameters,"** Proc. American Control Conf., San Diego, CA, 1999, pp. 3784-3789.

[29] C. Canudas de Wit and P. Lischinsky, **"Adaptive friction compensation with dynamic friction model,"** in IFAC., San Francisco, CA, 1996, pp. 197-202.

[30] H.T. Goh et al., **"Modeling and compensation of pivot friction in a disk drive actuator,"** in ACC., Seattle, WA, 1995, pp. 4141-4145.

[31] K.J. Astrom and B. Wittenmark, **"A survey of adaptive control application,"** Proc. 34th Conf. on Decision and Control, New Orleans, LA, 1995, pp. 649-654.

REFERENCES (CONT.)

[32] R. Horowitz and B. Li, **"Adaptive control for disk file actuators,"** Proc. 34th Conf. on Decision and Control, 1995, pp. 655-660.

[33] R. Horowitz and B. Li, **"Design and implementation of adaptive non-repetitive track-following disk file servos,"** Proc. 1995 American Control Conference, 1995, pp. 4161-4166.

[34] R. Horowitz and Bo Li, **"Adaptive track-following servos for disk file actuators,"** IEEE Transactions on Magnetics, vol. 7, no. 6, pp. 525-546, 1996.

[35] R. Horowitz et al., **"Adaptive track following servos for disk files,"** Proc. 13th World Congress, International Federation of Automatic Control, San Francisco, CA, 1996, pp. 495-500.

[36] B. Yao et al., **"General high performence adaptive robust control of machine tools,"** Proc. Advanced Intelligent Mechatronics, Tokyo, Japan, 1997.

[37] B. Yao et al., **"High performance robust motion control of machine tools: an adaptive robust control approach and comparative experiments,"** Proc. ACC, 1997.

[38] B. Yao and M. Tomizuka, **"Smooth robust adaptive sliding mode control of robot manipulators with guaranteed tranisent performence,"** Proc. Advanced Intelligent Mechatronics, 1994, pp. 1176-1180.

[39] B Yao et al., **"High-performance robust motion control of machine tools: an adaptive robust control approach and comparative experiments,"** IEEE/ASME Trans. Mechatron., vol.2, no. 2, pp. 63-76, 1997.

[40] W. Chatlatanagulchai and K. Prasertsom, **"Hard Disk Drive Dual-Stage Actuator Track Following Control Using Two Degrees-of-Freedom H-infinity Loop Shaping,"** in Journal of Research in Engineering and Technology, Kasetsart University, 2008.

REFERENCES (CONT.)

[41] R. Galindo, **"Mixed Sensitivity H-infinity Control of a Three-Tank-System,"** in American Control Conference, Porland, OR, Jun 2005.

[42] H. Patel. (2014, Mar. 3). **"Hard Drive History & Information,"** [Online]. Available: http://hddinfo2010.blogspot.com.

[43] J. Nie and R. Horowitz, **"A Tutorial on Control Design of Hard Disk Drive Self-Servo Track Writing,"** The work was supported in part by the Information Storage Industry Consortium and the Computer Mechanics Laboratory at UC Berkeley, 2009.

[44] L. Yi., **"Two Degree of Freedom Control for Disk Drive Servo Systems,"** Ph.D. dissertation. Univ. California, Berkeley, 2000.

[45] GetData Software Development company. (2014, Mar. 3). **"Data Recovery Basic,"** [Online]. Available: http://www.recovermyfiles.com/data-recovery-help/fundamentals.php.

[46] R. Ehrich, **"Tpi growth is key to delaying superparamagnetism's arrival,"** in Data Storage, vol. 6, no. 10, 1999.

[47] B.M. Chen et al., **"Hard Disk Drive Servo Systems,"** 2nd ed. London: Springer, 2006, pp. 310.

[48] A.H. Sacks et al., **"Advanced methods for repeatable runout compensation,"** IEEE Trans. Magn., vol. 31, pp. 1031-1036, 1995.

[49] G.F. Franklin et al., **"Digital control of dynamic systems,"** 3rd ed. Reading. MA: Addison-Wesley, 1998.

[50] G. Jamg et al., **"New frequency domain method of nonrepeatable runout measurement in a hard disk drive spindle motor,"** IEEE Trans. Magn., vol.35, pp. 833-838, 1999.

[51] D. Abramovitch et al., **"An overview of the PES Pareto method for decomposing baseline noise sources in hard disk position error signals,"** IEEE Trans. Magn., vol. 34, pp17-23, 1998.

REFERENCES (CONT.)

[52] Q. Li et al., **"Analysis of the dynamics of 3.5 hard disk drive actuators,"** in Data Storage Inst., Singapore, 1997.

[53] S. Zeng et al., **"Novel method for minimizing track seeking residual vibrations of hard disk drives,"** IEEE Trans. Magn., vol. 37, pp. 1146-1156, 2001.

[54] Y.A. Mah, **"Design of a high bandwidth moving-coil actuator with force couple actuation,"** IEEE Trans. Magn., vol. 35, pp. 874-878, 1999.

[55] J.S. McAllister, **"The effect of disk platter resonances on track misregistration in 3.5 disk drives,"** IEEE Trans. Magn., vol.35, pp. 1762-1766, 1996.

[56] H. Hanselmann and W. Mortix, **"High-bandwidth control of the head positioning mechanism in a winchester disk drive,"** IEEE Control. Syst. Mag., vol. 7, pp. 15-19, 1987.

[57] G. Guo, **"Lecture notes in servo engineering,"** Dept. Elect. and Comp. Eng., National Univ., Singapore, 1998.

[58] P.A. Weaver and R.M. Ehrlich, **"The use of multirate notch filters in embedded servo disk drives,"** Proc. American Contr. Conf., San Francisco, CA, 1993, pp. 4156-4160.

[59] G.F. Franklin et al., **"Digital Control of Dynamic Systems,"** 2nd ed. Anderson Wesley, 1990.

[60] T. Yamaguchi et al., **"A mode-switching control for motion control and its application to disk drives: design of optimal model-switching conditions,"** IEEE/ASME Trans. Mechatron., vol. 3, pp. 202-209, 1998.

[61] S.S. Nair, **"Automatic Weight Selection Algorithm for Designing H Infinity controller for Active Magnetic Bearing,"** in International Journal of Engineering Science and Technology (IJEST), vol. 3, no. 1 Jan 2011.

[62] W. Beaven et al., **"Weighting Function selection in the H_∞ design process,"** in Control Eng. practice, vol. 4, no. 5, pp. 625-633, 1996.

REFERENCES (CONT.)

[63] G. Cao et al., **"The Characteristics Analysis of Magnetic Bearing Basedon H-infinity Controller,"** Proc. 51th World Congress on Intelligent Control and Automation, Hangzhou, P.R. China, Jun. 2004.

[64] Arredondo and J. Jugo, **"Active Magnetic Bearings Robust Control Design based on Symmetry Properties,"** Proc. 2007 American Control Conf., USA, Jul. 2007.

[65] Z. Gosiewski and A. Mystokowski, **"Robust control of active magnetic bearing suspension: Analytical and experimental study,"** in Mechanical systems and Signal Processing, 2007.

[66] J. Hu et al., **"Systematic H_∞ weighting function selection and its application to the real-time control of a vertical take-off aircraft,"** in Control Eng. Practice, vol. 8, 2000, pp. 241-252.

[67] C.R. Knospe, **"Active magnetic bearings for machining applications,"** Control Eng. Practice 15, 2007, pp. 307–313.

[68] G. Balas, et al., **"Robust Control Toolbox 3 User's Guide,"** Apr. 2009.

[69] M.G. Ortega and F.R. Rubio. **"Systematic design of weighting matrices for the H_∞ mixed sensitivity problem,"** in Journal of Process Control, vol. 14, 2004, pp. 89-98.

[70] J.C. Doyle et al., **"State-space solutions to standard H2 and H_∞ control problems,"** IEEE Trans. Autom. Control, vol. 34, no.8, pp. 831-847, 1989.

[71] P. Iglesias and K. Glover. **"State-space approach to discrete-time H_∞ control,"** in International Journal of Control, vol. 54, no. 5, 1991, pp. 1031–1073.

[72] G. Balas et al., **"m-Analysis and Synthesis Toolbox User's Guide,"** 2nd ed., The MathWorks, Natick, MA, 1995.

[73] R. Chiang and M. Safonov, **"Robust Control Toolbox User's Guide,"** 2nd ed., The MathWorks, Natick, MA, 1998.

[74] S. Skogestad and I. Postlethwaite, **"Multivariable Feedback Control Analysis and Design,"** NY: John Wiley & Sons, 1996.

[75] K. Zhou et al., **"Robust and Optimal Control,"** NJ: Prentice-Hall, 1996.

APPENDIX

```
%-------------------------------------------------------------------------------------------------------------

%       Track-Following Control of HDD Actuator Using H-infinity Mixed-Sensitivity Control

%-------------------------------------------------------------------------------------------------------------

% Code:     Tanapol Kaew-Arunyik

% Advisor : Assoc.Dr.Withit Chatlatanakulchai

%-------------------------------------------------------------------------------------------------------------

clear

close all

clc

s=tf('s');

%---------------------------------- Time Domain Parameters ----------------------------------

ts = 1/(20e3);  %sampling time 20 kHz

tend = 0.03     %End Time 30 ms

t = 0:ts:tend;

%---------------------------------- Natural Frequency Mode (Gr) ----------------------------------

Gr1 = (0.912*s^2+(457.4*s)+1.433e8)/(s^2+359.2*s+1.433e8);

Gr2 = (0.7586*s^2+962.2*s+2.491e8)/(s^2+789.1*s+2.491e8);

Gr3 = 9.917e8/(s^2+1575*s+9.917e8);

Gr4 = 2.731e9/(s^2+2613*s+2.731e9);

%---------------------------------------- Notch Filter(Gn)----------------------------------------

Gn1 = (s^2+238.8*s+1.425e8)/(s^2+2388*s+1.425e8);
```

```
Gn2 = (s^2+314.2*s+2.467e8)/(s^2+3142*s+2.467e8);

Gn3 = (s^2+628.3*s+9.87e8)/(s^2+12570*s+9.87e8);

%---------------------------------------------- VCM Plant ----------------------------------------------

Gv = 6.4013e7/((s+0.0001)^2);

Gn = Gn1*Gn2*Gn3;

Gr = Gr1*Gr2*Gr3*Gr4;

G = (Gv*Gr);

%---------------------------------------------- Bode Plot ----------------------------------------------

%Plot G and Gn

figure('Name','Plant G','NumberTitle','on'),Bode(G, 'g-.', G*Gn, 'g'); grid on; legend('VCM
plant','VCM plant with Filter',1,2);

figure('Name','Notch Filter Gn','NumberTitle','on'),Bode(Gn,{2*pi*1e2,2*pi*1e4}); grid on;

%----------------------------------------Weight Functions Design----------------------------------------

%Params Setting

wb=2*pi*500     % desired closed-loop bandwidth

A=1/100;  % desired disturbance attenuation inside bandwidth

M=2 ;      % desired bound on hinfnorm(S) & hinfnorm(T)


W1=(s/M+wb)/(s+wb*A); % Sensitivity weight

W2=[];                % KS, Empty control weight

W3=(0.735*s+wb/M)/(A*s+wb); % Complementary sensitivity weight

figure('Name','Weight
Functions','NumberTitle','on'),subplot(211),sigmaplot(inv(W1)),subplot(212),sigmaplot(inv(W3));
```

```
%-----------------Synthesize K using H-infinity Mixed-Sensitivity (S/T configuration)----------------

[K,CL,GAM,INFO]=mixsyn(Gv,W1,W2,W3);

%---------------------- Finding Sensitivity(S) and Its Complementary(T) Function ---------------------

L=G*Gn*K  % loop transfer function

S=inv(1+L); % Sensitivity

T=1-S;      % complementary sensitivity

figure('Name','shapes sigma plots','NumberTitle','on'),sigma(GAM/W1,'--r',GAM/W3,'--b',S,'-r',T,'-
b');legend('GAM/Ws','GAM/Wt','S','T',2);

figure('Name','Singular Value of |S|+|T|','NumberTitle','on'),sigma(S,T);

%------------------------------------------ Phase/Gain Margin ------------------------------------------

[Gm, Pm, Wgm, Wpm] = margin(L);

SS = allmargin(L)

figure('Name','Bode of Closed-loop','NumberTitle','on'), Bode(L,{0.1,25000}); grid on;

figure('Name','Margin','NumberTitle','on'),margin(L);

%-------------------------------------------- Plot S and T ---------------------------------------------

%------------------------------ Sensitivity and Its Complementary Function----------------------------

r = square(2*pi*0.1*t);

yd = lsim(S,r,t); %disturbance rejection

y = lsim(T,r,t); %tracking

figure('Name','y = lsim()...tracking','NumberTitle','on')

subplot(221),plot(t,y),hold on,plot(t,r,':');

grid on;
```

```
subplot(222),plot(t,yd),hold on,plot(t,r,':')

grid on;

hold off;

u = lsim(K*S,r,t); %control input

figure('Name','u = lsim()...control input','NumberTitle','on')

subplot(221),plot(t,u)

%----------------------------------------Design Benchmark----------------------------------------

%                                    time-domain simulation

%                                tracking and disturbance rejection

%------------------------------------------------------------------------------------------------

r = square(2*pi*(1/1e-2)*t); %reference

d = 0.1*sin(110*pi*t) + 0.05*sin(220*pi*t) + 0.02*sin(440*pi*t) + 0.01*sin(880*pi*t); %plant-
output disturbance

n = sqrt(9e-6)*randn(length(t),1); %noise

y = lsim(T,r,t) + lsim(S,d,t) + lsim(-T,n,t);

yr = lsim(T,r,t);

yd = lsim(S,d,t);

yn = lsim(-T,n,t);


figure('Name', 'Disturbance/Noise Atttenuation & Tracking Performance', 'NumberTitle', 'on')

subplot(411), plot(t,r,'--',t,0.95*r,'--',t,1.05*r,'--',t,y,'-')

subplot(412), plot(t,r,'--',t,yr,'-')
```

```
subplot(413), plot(t,d,'--',t,yd,'-')

subplot(414), plot(t,n,'-',t,yn,'-')


%control effort

u = lsim(K*S,r-d,t);

figure('Name', 'Control efforts', 'NumberTitle', 'on'), plot(t,u)

GAM

Gm

Gm_dB = 20*log10(Gm)

Pm

Wgm

Wpm

INFO
```

AUTHOR BIOGRAPHY

Name	Mr. Tanapol Kaew-Arunyik
Date of Birth	July 3, 1984
Place of Birth	Nakorn-Ratchasima, Thailand
Education	2006 B. Eng. In Computer Engineering, Thammasat University
Scholarship	2008-2010 Master Scholarship in Data Storage Technology, The National Electronics and Computer Technology Center and Seagate Technology
Knowledge Taxonomy	- Embedded System - Automatic Control - Automation Technology - Data Storage Technology
Work Experience	- 2006-2007 Factory Information System Engineer at Seagate Technology - 2007-2008 Network Engineer at Seagate Technology - 2008-2011 HDD Failure Analysis Engineer at Seagate Technology - 2011-2014 Automation Software Engineer at Seagate Technology